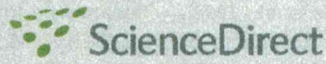


- Zeher, A. M.; Dimmeler, S.; Henze, E. 111In-labeled CD34+ hematopoietic progenitor cells in a rat myocardial infarction model. *J. Nucl. Med.* 45(3):512–518; 2004.
12. Callera, F.; de Melo, C. M. Magnetic resonance tracking of magnetically labeled autologous bone marrow CD34+ cells transplanted into the spinal cord via lumbar puncture technique in patients with chronic spinal cord injury: CD34+ cells' migration into the injured site. *Stem Cells Dev.* 16(3):461–466; 2007.
 13. Cao, Q. L.; Zhang, Y. P.; Howard, R. M.; Walters, W. M.; Tsoulfas, P.; Whitemore, S. R. Pluripotent stem cells engrafted into the normal or lesioned adult rat spinal cord are restricted to a glial lineage. *Exp. Neurol.* 167(1): 48–58; 2001.
 14. Cho, S. R.; Kim, Y. R.; Kang, H. S.; Yim, S. H.; Park, C. I.; Min, Y. H.; Lee, B. H.; Shin, J. C.; Lim, J. B. Functional recovery after the transplantation of neurally differentiated mesenchymal stem cells derived from bone marrow in a rat model of spinal cord injury. *Cell Transplant.* 18(12):1359–1368; 2009.
 15. Chow, S. Y.; Moul, J.; Tobias, C. A.; Himes, B. T.; Liu, Y.; Obrocka, M.; Hodge, L.; Tessler, A.; Fischer, I. Characterization and intraspinal grafting of EGF/bFGF-dependent neurospheres derived from embryonic rat spinal cord. *Brain Res.* 874(2):87–106; 2000.
 16. Cloutier, F.; Siegenthaler, M. M.; Nistor, G.; Keirstead, H. S. Transplantation of human embryonic stem cell-derived oligodendrocyte progenitors into rat spinal cord injuries does not cause harm. *Regen. Med.* 1(4):469–479; 2006.
 17. Contag, C. H.; Bachmann, M. H. Advances in in vivo bioluminescence imaging of gene expression. *Annu. Rev. Biomed. Eng.* 4:235–260; 2002.
 18. Coutts, M.; Keirstead, H. S. Stem cells for the treatment of spinal cord injury. *Exp. Neurol.* 209(2):368–377; 2008.
 19. Cummings, B. J.; Uchida, N.; Tamaki, S. J.; Salazar, D. L.; Hooshmand, M.; Summers, R.; Gage, F. H.; Anderson, A. J. Human neural stem cells differentiate and promote locomotor recovery in spinal cord-injured mice. *Proc. Natl. Acad. Sci. USA* 102(39):14069–14074; 2005.
 20. de Haro, J.; Zurita, M.; Ayllon, L.; Vaquero, J. Detection of 111In-oxine-labeled bone marrow stromal cells after intravenous or intralesional administration in chronic paraplegic rats. *Neurosci. Lett.* 377(1):7–11; 2005.
 21. Eaton, M. J.; Wolfe, S. Q.; Martinez, M.; Hernandez, M.; Furst, C.; Huang, J.; Frydel, B. R.; Gomez-Marin, O. Subarachnoid transplant of a human neuronal cell line attenuates chronic allodynia and hyperalgesia after excitotoxic spinal cord injury in the rat. *J. Pain* 8(1):33–50; 2007.
 22. Edinger, M.; Cao, Y. A.; Hornig, Y. S.; Jenkins, D. E.; Vermeris, M. R.; Bachmann, M. H.; Negrin, R. S.; Contag, C. H. Advancing animal models of neoplasia through in vivo bioluminescence imaging. *Eur. J. Cancer* 38(16): 2128–2136; 2002.
 23. Gal, P.; Kravcukova, P.; Mokry, M.; Kluchova, D. Chemokines as possible targets in modulation of the secondary damage after acute spinal cord injury: A review. *Cell. Mol. Neurobiol.* 29(6–7):1025–1035; 2009.
 24. Gao, J.; Dennis, J. E.; Muzic, R. F.; Lundberg, M.; Caplan, A. I. The dynamic in vivo distribution of bone marrow-derived mesenchymal stem cells after infusion. *Cells Tissues Organs* 169(1):12–20; 2001.
 25. Hara, M.; Murakami, T.; Kobayashi, E. In vivo bioimaging using photogenic rats: Fate of injected bone marrow-derived mesenchymal stromal cells. *J. Autoimmun.* 30(3): 163–171; 2008.
 26. Hoehn, M.; Kustermann, E.; Blunk, J.; Wiedermann, D.; Trapp, T.; Wecker, S.; Focking, M.; Arnold, H.; Hescheler, J.; Fleischmann, B. K.; Schwandt, W.; Buhle, C. Monitoring of implanted stem cell migration in vivo: A highly resolved in vivo magnetic resonance imaging investigation of experimental stroke in rat. *Proc. Natl. Acad. Sci. USA* 99(25):16267–16272; 2002.
 27. Hofstetter, C. P.; Holmstrom, N. A.; Lilja, J. A.; Schweinhardt, P.; Hao, J.; Spenger, C.; Wiesenfeld-Hallin, Z.; Kurpad, S. N.; Frisen, J.; Olson, L. Allodynia limits the usefulness of intraspinal neural stem cell grafts; directed differentiation improves outcome. *Nat. Neurosci.* 8(3):346–353; 2005.
 28. Iwanami, A.; Kaneko, S.; Nakamura, M.; Kanemura, Y.; Mori, H.; Kobayashi, S.; Yamasaki, M.; Momoshima, S.; Ishii, H.; Ando, K.; Tanioka, Y.; Tamaoki, N.; Nomura, T.; Toyama, Y.; Okano, H. Transplantation of human neural stem cells for spinal cord injury in primates. *J. Neurosci. Res.* 80(2):182–190; 2005.
 29. Jendelova, P.; Herynek, V.; Urdzikova, L.; Glogarova, K.; Kroupova, J.; Andersson, B.; Bryja, V.; Burian, M.; Hajek, M.; Sykova, E. Magnetic resonance tracking of transplanted bone marrow and embryonic stem cells labeled by iron oxide nanoparticles in rat brain and spinal cord. *J. Neurosci. Res.* 76(2):232–243; 2004.
 30. Keirstead, H. S.; Nistor, G.; Bernal, G.; Totoiu, M.; Cloutier, F.; Sharp, K.; Steward, O. Human embryonic stem cell-derived oligodendrocyte progenitor cell transplants remyelinate and restore locomotion after spinal cord injury. *J. Neurosci.* 25(19):4694–4705; 2005.
 31. Khalatbary, A. R.; Tiraihi, T. Localization of bone marrow stromal cells in injured spinal cord treated by intravenous route depends on the hemorrhagic lesions in traumatized spinal tissues. *Neurol. Res.* 29(1):21–26; 2007.
 32. Kim, B. G.; Hwang, D. H.; Lee, S. I.; Kim, E. J.; Kim, S. U. Stem cell-based cell therapy for spinal cord injury. *Cell Transplant.* 16(4):355–364; 2007.
 33. Kumagai, G.; Okada, Y.; Yamane, J.; Nagoshi, N.; Kitamura, K.; Mukaino, M.; Tsuji, O.; Fujiyoshi, K.; Katoh, H.; Okada, S.; Shibata, S.; Matsuzaki, Y.; Toh, S.; Toyama, Y.; Nakamura, M.; Okano, H. Roles of ES cell-derived gliogenic neural stem/progenitor cells in functional recovery after spinal cord injury. *PLoS ONE* 4(11): e7706; 2009.
 34. Lee, J.; Kuroda, S.; Shichinohe, H.; Ikeda, J.; Seki, T.; Hida, K.; Tada, M.; Sawada, K.; Iwasaki, Y. Migration and differentiation of nuclear fluorescence-labeled bone marrow stromal cells after transplantation into cerebral infarct and spinal cord injury in mice. *Neuropathology* 23(3):169–180; 2003.
 35. Lee, Z.; Dennis, J. E.; Gerson, S. L. Imaging stem cell implant for cellular-based therapies. *Exp. Biol. Med.* (Maywood) 233(8):930–940; 2008.
 36. Lepore, A. C.; Bakshi, A.; Swanger, S. A.; Rao, M. S.; Fischer, I. Neural precursor cells can be delivered into the injured cervical spinal cord by intrathecal injection at the lumbar cord. *Brain Res.* 1045(1–2):206–216; 2005.
 37. McDonald, J. W.; Liu, X. Z.; Qu, Y.; Liu, S.; Mickey, S. K.; Turetsky, D.; Gottlieb, D. I.; Choi, D. W. Transplanted embryonic stem cells survive, differentiate and promote recovery in injured rat spinal cord. *Nat. Med.* 5(12):1410–1412; 1999.

38. Mikami, Y.; Okano, H.; Sakaguchi, M.; Nakamura, M.; Shimazaki, T.; Okano, H. J.; Kawakami, Y.; Toyama, Y.; Toda, M. Implantation of dendritic cells in injured adult spinal cord results in activation of endogenous neural stem/progenitor cells leading to de novo neurogenesis and functional recovery. *J. Neurosci. Res.* 76(4):453–465; 2004.
39. Morikawa, S.; Mabuchi, Y.; Kubota, Y.; Nagai, Y.; Niibe, K.; Hiratsu, E.; Suzuki, S.; Miyauchi-Hara, C.; Nagoshi, N.; Sunabori, T.; Shimmura, S.; Miyawaki, A.; Nakagawa, T.; Suda, T.; Okano, H.; Matsuzaki, Y. Prospective identification, isolation, and systemic transplantation of multipotent mesenchymal stem cells in murine bone marrow. *J. Exp. Med.* 206(11):2483–2496; 2009.
40. Nagai, T.; Ibata, K.; Park, E. S.; Kubota, M.; Mikoshihba, K.; Miyawaki, A. A variant of yellow fluorescent protein with fast and efficient maturation for cell-biological applications. *Nat. Biotechnol.* 20(1):87–90; 2002.
41. Nakamura, M.; Bregman, B. S. Differences in neurotrophic factor gene expression profiles between neonate and adult rat spinal cord after injury. *Exp. Neurol.* 169(2):407–415; 2001.
42. Nakamura, M.; Okano, H.; Toyama, Y.; Dai, H. N.; Finn, T. P.; Bregman, B. S. Transplantation of embryonic spinal cord-derived neurospheres support growth of supraspinal projections and functional recovery after spinal cord injury in the neonatal rat. *J. Neurosci. Res.* 81(4):457–468; 2005.
43. Neuhuber, B.; Barshinger, A. L.; Paul, C.; Shumsky, J. S.; Mitsui, T.; Fischer, I. Stem cell delivery by lumbar puncture as a therapeutic alternative to direct injection into injured spinal cord. *J. Neurosurg. Spine* 9(4):390–399; 2008.
44. Ogawa, Y.; Sawamoto, K.; Miyata, T.; Miyao, S.; Watanabe, M.; Nakamura, M.; Bregman, B. S.; Koike, M.; Uchiyama, Y.; Toyama, Y.; Okano, H. Transplantation of in vitro-expanded fetal neural progenitor cells results in neurogenesis and functional recovery after spinal cord contusion injury in adult rats. *J. Neurosci. Res.* 69(6):925–933; 2002.
45. Ohta, M.; Suzuki, Y.; Noda, T.; Ejiri, Y.; Dezawa, M.; Kataoka, K.; Chou, H.; Ishikawa, N.; Matsumoto, N.; Iwashita, Y.; Mizuta, E.; Kuno, S.; Ide, C. Bone marrow stromal cells infused into the cerebrospinal fluid promote functional recovery of the injured rat spinal cord with reduced cavity formation. *Exp. Neurol.* 187(2):266–278; 2004.
46. Ohta, Y.; Takenaga, M.; Tokura, Y.; Hamaguchi, A.; Matsumoto, T.; Kano, K.; Mugishima, H.; Okano, H.; Igarashi, R. Mature adipocyte-derived cells, dedifferentiated fat cells (DFAT), promoted functional recovery from spinal cord injury-induced motor dysfunction in rats. *Cell Transplant.* 17(8):877–886; 2008.
47. Okada, S.; Ishii, K.; Yamane, J.; Iwanami, A.; Ikegami, T.; Katoh, H.; Iwamoto, Y.; Nakamura, M.; Miyoshi, H.; Okano, H. J.; Contag, C. H.; Toyama, Y.; Okano, H. In vivo imaging of engrafted neural stem cells: Its application in evaluating the optimal timing of transplantation for spinal cord injury. *FASEB J.* 19(13):1839–1841; 2005.
48. Okano, H. Stem cell biology of the central nervous system. *J. Neurosci. Res.* 69(6):698–707; 2002.
49. Okano, H.; Okada, S.; Nakamura, M.; Toyama, Y. Neural stem cells and regeneration of injured spinal cord. *Kidney Int.* 68:1927–1931; 2005.
50. Okano, H.; Sakaguchi, M.; Ohki, K.; Suzuki, N.; Sawamoto, K. Regeneration of the central nervous system using endogenous repair mechanisms. *J. Neurochem.* 102(5):1459–1465; 2007.
51. Parr, A. M.; Kulbatski, I.; Tator, C. H. Transplantation of adult rat spinal cord stem/progenitor cells for spinal cord injury. *J. Neurotrauma* 24(5):835–845; 2007.
52. Parr, A. M.; Tator, C. H.; Keating, A. Bone marrow-derived mesenchymal stromal cells for the repair of central nervous system injury. *Bone Marrow Transplant.* 40(7):609–619; 2007.
53. Partlow, K. C.; Chen, J.; Brant, J. A.; Neubauer, A. M.; Meyerrose, T. E.; Creer, M. H.; Nolte, J. A.; Caruthers, S. D.; Lanza, G. M.; Wickline, S. A. 19F magnetic resonance imaging for stem/progenitor cell tracking with multiple unique perfluorocarbon nanobeacons. *FASEB J.* 21(8):1647–1654; 2007.
54. Paul, C.; Samdani, A. F.; Betz, R. R.; Fischer, I.; Neuhuber, B. Grafting of human bone marrow stromal cells into spinal cord injury: A comparison of delivery methods. *Spine* 34(4):328–334; 2009.
55. Reynolds, B. A.; Tetzlaff, W.; Weiss, S. A multipotent EGF-responsive striatal embryonic progenitor cell produces neurons and astrocytes. *J. Neurosci.* 12(11):4565–4574; 1992.
56. Rice, B. W.; Cable, M. D.; Nelson, M. B. In vivo imaging of light-emitting probes. *J. Biomed. Opt.* 6(4):432–440; 2001.
57. Rolls, A.; Shechter, R.; Schwartz, M. The bright side of the glial scar in CNS repair. *Nat. Rev. Neurosci.* 10(3):235–241; 2009.
58. Rowland, J. W.; Hawryluk, G. W.; Kwon, B.; Fehlings, M. G. Current status of acute spinal cord injury pathophysiology and emerging therapies: Promise on the horizon. *Neurosurg. Focus* 25(5):E2; 2008.
59. Saito, F.; Nakatani, T.; Iwase, M.; Maeda, Y.; Hirakawa, A.; Murao, Y.; Suzuki, Y.; Onodera, R.; Fukushima, M.; Ide, C. Spinal cord injury treatment with intrathecal autologous bone marrow stromal cell transplantation: The first clinical trial case report. *J. Trauma* 64(1):53–59; 2008.
60. Sher, F.; van Dam, G.; Boddeke, E.; Copray, S. Bioluminescence imaging of Olig2-neural stem cells reveals improved engraftment in a demyelination mouse model. *Stem Cells* 27(7):1582–1591; 2009.
61. Sykova, E.; Jendelova, P. Magnetic resonance tracking of implanted adult and embryonic stem cells in injured brain and spinal cord. *Ann. NY Acad. Sci.* 1049:146–160; 2005.
62. Sykova, E.; Jendelova, P.; Urdzikova, L.; Lesny, P.; Hejcl, A. Bone marrow stem cells and polymer hydrogels—two strategies for spinal cord injury repair. *Cell. Mol. Neurobiol.* 26(7–8):1113–1129; 2006.
63. Takeuchi, H.; Natsume, A.; Wakabayashi, T.; Aoshima, C.; Shimato, S.; Ito, M.; Ishii, J.; Maeda, Y.; Hara, M.; Kim, S. U.; Yoshida, J. Intravenously transplanted human neural stem cells migrate to the injured spinal cord in adult mice in an SDF-1- and HGF-dependent manner. *Neurosci. Lett.* 426(2):69–74; 2007.
64. Tator, C. H. Review of treatment trials in human spinal cord injury: Issues, difficulties, and recommendations. *Neurosurgery* 59(5):957–987; 2006.
65. Thuret, S.; Moon, L. D.; Gage, F. H. Therapeutic interventions after spinal cord injury. *Nat. Rev. Neurosci.* 7(8):628–643; 2006.
66. Togel, F.; Yang, Y.; Zhang, P.; Hu, Z.; Westenfelder, C. Bioluminescence imaging to monitor the in vivo distribu-

- tion of administered mesenchymal stem cells in acute kidney injury. *Am. J. Physiol. Renal Physiol.* 295(1):F315–321; 2008.
67. Vaquero, J.; Zurita, M.; Oya, S.; Santos, M. Cell therapy using bone marrow stromal cells in chronic paraplegic rats: Systemic or local administration? *Neurosci. Lett.* 398(1–2):129–134; 2006.
68. Whetstone, W. D.; Hsu, J. Y.; Eisenberg, M.; Werb, Z.; Noble-Haeusslein, L. J. Blood–spinal cord barrier after spinal cord injury: Relation to revascularization and wound healing. *J. Neurosci. Res.* 74(2):227–239; 2003.
69. Wu, S.; Suzuki, Y.; Noda, T.; Bai, H.; Kitada, M.; Kataoka, K.; Nishimura, Y.; Ide, C. Immunohistochemical and electron microscopic study of invasion and differentiation in spinal cord lesion of neural stem cells grafted through cerebrospinal fluid in rat. *J. Neurosci. Res.* 69(6): 940–945; 2002.
70. Yoshihara, T.; Ohta, M.; Itokazu, Y.; Matsumoto, N.; Dezawa, M.; Suzuki, Y.; Taguchi, A.; Watanabe, Y.; Adachi, Y.; Ikehara, S.; Sugimoto, H.; Ide, C. Neuroprotective effect of bone marrow-derived mononuclear cells promoting functional recovery from spinal cord injury. *J. Neurotrauma* 24(6):1026–1036; 2007.

available at www.sciencedirect.comwww.elsevier.com/locate/brainres

**BRAIN
RESEARCH**

Research Report

Feasibility study for functional test battery of SOD transgenic rat (H46R) and evaluation of edaravone, a free radical scavenger

Masashi Aoki^{a,b}, Hitoshi Warita^{a,b}, Hideki Mizuno^{a,b}, Naoki Suzuki^{a,b}, Satoshi Yuki^{c,*}, Yasuto Itoyama^d

^aDepartment of Neurology, Tohoku University School of Medicine, Sendai, Miyagi, Japan

^bTohoku University Hospital ALS Center, Sendai, Miyagi, Japan

^cPharmacology Research Laboratories I, Mitsubishi Tanabe Pharma Corporation, Yokohama, Kanagawa, Japan

^dNational Center Hospital, National Center of Neurology and Psychiatry, Kodaira, Tokyo, Japan

ARTICLE INFO

Article history:

Accepted 19 January 2011

Available online 26 January 2011

Keywords:

Amyotrophic lateral sclerosis

SOD1

Transgenic rats

Free radical

ABSTRACT

We evaluated a battery of functional tests for investigating the effects of edaravone, a free radical scavenger, in SOD1 transgenic (H46R) rat model of amyotrophic lateral sclerosis. Edaravone (1.5 or 3.0 mg/kg/h) or saline was administered intravenously to rats by continuous infusion (1 h per day) for 2 days, followed by a 2-day holiday. Lifetime and duration of illness were evaluated, and motor function was assessed using the hind-foot reflex test, landing foot-splay test, rota rod test and inclined plate test at a predetermined time point at which half of the control animals had died. Statistical comparison of motor functions of edaravone-treated and control SOD1 transgenic rats at an objectively determined time point was confirmed to be feasible. Edaravone-treated male rats showed significantly better performance in the landing foot-splay test. The present model seems suitable for evaluating motor function of H46R SOD1 transgenic rats, and be useful for examining the therapeutic potential of edaravone to treat amyotrophic lateral sclerosis.

© 2011 Elsevier B.V. All rights reserved.

1. Introduction

Amyotrophic lateral sclerosis (ALS) is a neurodegenerative disorder which affects motor neurons in the central nervous system. Little is known about its cause, though 5% to 10% of all ALS is familial (FALS), and of these patients, about 20% have mutation in the Cu/Zn superoxide dismutase (SOD1) gene (Rosen et al., 1993; Aoki et al., 1993). However, many of these mutations have little effect on the enzymatic activity of SOD1.

SOD1-deficient mice do not develop a degenerative ALS-like phenotype (Reaume et al., 1996), but mice that express

human mutant SOD1 in addition to endogenous wild-type mouse SOD1 do develop ALS-like symptoms (Gurney et al., 1994). These findings suggest that motor neuron death is triggered by a gain of toxic function. It has been suggested that this toxic gain-of-function of mutant SODs enhances oxidative activity, increasing the production of hydroxyl radical or peroxynitrite; in other words, it is hypothesized that free radicals contribute to ALS pathogenesis.

Edaravone (3-methyl-1-phenyl-2-pyrazolin-5-one) is a free radical scavenger approved in Japan, and widely used for the treatment of acute cerebral infarction (The Edaravone Acute

* Corresponding author at: Pharmacology Research Laboratories I, Mitsubishi Tanabe Pharma Corporation, Yokohama, Kanagawa, 227-0033, Japan. Fax: +81 45 963 4641.

E-mail address: yuki.satoshi@mg.mt-pharma.co.jp (S. Yuki).

Infarction Study Group, 2003). It is well known that edaravone scavenges hydroxyl radicals and inhibits lipid peroxidation (Abe et al., 1988; Watanabe et al., 1994; Mizuno et al., 1998). These reports encouraged us to investigate the effects of edaravone in a rat model of ALS expressing a human SOD1 transgene with ALS-associated mutation: histidine to arginine at position 46 (H46R) (Nagai et al., 2001). This transgenic rat displays adult onset of symptoms, slower progression and less variability in the phenotype than Gly93Ala (G93A) transgenic rat (Nagai et al., 2001; Matsumoto et al., 2006).

The motor functional assessments we selected for this study were the hind-foot reflex test, landing foot-splay test, rota rod test and inclined plate test. This battery of assessments allows us to evaluate a range of motor functions, including reflex function, coordinated movement and muscular strength. For statistical comparisons of functional assessment outcomes, we used a predetermined evaluation time point by which half of the control animals had died; this provides an objective way to determine the evaluation time point.

Edaravone was administered by continuous infusion (1 h per day) for 2 days followed by a 2-day holiday from 18 weeks of age to the day of loss of righting reflex. This dosing regime is similar to those used ongoing Phase III clinical study in ALS patients in Japan.

The purposes of this study were to see whether our battery of functional tests represents a reasonable choice for evaluation of this SOD1 (H46R) transgenic rat model and to make a preliminary examination of the effect of edaravone, a free radical scavenger.

2. Results

Three animals (one male in the edaravone high-dose group, one female in the edaravone low-dose group and one female in the edaravone high-dose group) were excluded because forelimb paralysis was observed before hind-limb paralysis. The day by which half of the control animals had died was day 194 for males and day 208 for females.

2.1. Lifetime and the duration of illness

The mean lifetimes of animals in the control, edaravone low-dose and edaravone high-dose groups were 196 ± 3 , 200 ± 1 and

202 ± 4 days for males, and 212 ± 4 , 214 ± 5 and 224 ± 10 days for females, respectively. Durations of illness in the control, edaravone low-dose and edaravone high-dose groups were 52.0 ± 3.2 , 54.3 ± 2.1 and 57.6 ± 5.2 for males and 67.6 ± 4.6 , 72.1 ± 4.6 and 78.7 ± 10.5 for females, respectively. Edaravone dose-dependently increased both the lifetime and duration of illness, although the changes did not reach statistical significance (Fig. 1).

2.2. Motor functional assessments

2.2.1. Hind-foot reflex test

The evaluation time point in the hind-foot reflex test was 194 days for males and 208 days for females. The mean scores of the control, edaravone low-dose and edaravone high-dose groups were 3.3 ± 0.3 , 3.1 ± 0.1 and 2.6 ± 0.3 for males, and 3.5 ± 0.3 , 2.9 ± 0.3 and 3.0 ± 0.4 females, respectively. The differences were not statistically significant (Table 1).

2.2.2. Landing foot-splay test

The evaluation time point in the hind-foot reflex test was 190 days for males and 204 days for females. The mean landing foot-splay distances between the hind feet in the control, edaravone low-dose and edaravone high-dose groups were 3.4 ± 0.8 , 3.0 ± 0.4 and 5.6 ± 0.5 cm for males, and 3.3 ± 0.4 , 4.2 ± 0.6 and 4.4 ± 0.4 cm for females, respectively. The high-dose edaravone-treated male group showed a significant improvement ($p < 0.05$ vs. control group, Dunnett's test) (Table 1, Fig. 2).

2.2.3. Rota rod test

The evaluation time point in the rota rod test was 193 days for males and 207 days for females. The mean values of the longest time for which the animals could remain on the rod before falling in the control, edaravone low-dose and edaravone high-dose groups were 2.5 ± 0.8 , 1.0 ± 0.0 and 3.3 ± 1.5 s for males, and 4.0 ± 1.8 , 2.7 ± 0.4 and 13.1 ± 8.2 s for females, respectively. The differences were not statistically significant (Table 1).

2.2.4. Inclined plate test

The evaluation time point in the inclined plate test was 192 days for males and 208 days for females. The values of the mean angle that the animals could sustain without slipping in

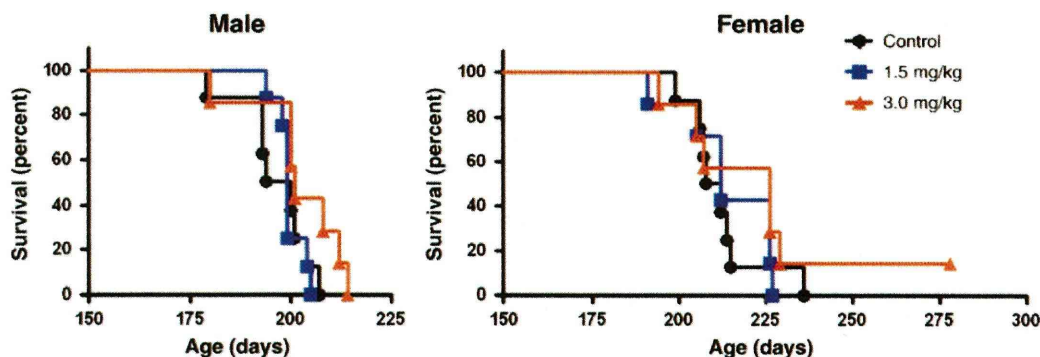


Fig. 1 – Kaplan–Meier survival plots. No significant difference was observed. (Log-rank test followed by Holm's multiple comparison test.)

Table 1 – Effect of edaravone on motor functions in H46R SOD transgenic rats.

	Male	n	Evaluation point (day)	Female	n	Evaluation point (day)
Hind-foot reflex test						
Control	3.3±0.3	8	194	3.5±0.3	8	208
Edaravone 1.5 mg/kg/h	3.1±0.1 (p=0.7811)	8		2.9±0.3 (p=0.2627)	7	
Edaravone 3.0 mg/kg/h	2.6±0.3 (p=0.2412)	7		3.0±0.4 (p=0.4938)	7	
Landing foot-splay test (cm)						
Control	3.4±0.8	8	190	3.3±0.4	8	204
Edaravone 1.5 mg/kg/h	3.0±0.4 (p=0.8073)	8		4.2±0.6 (p=0.3141)	7	
Edaravone 3.0 mg/kg/h	5.6±0.5* (p=0.0477)	7		4.4±0.4 (p=0.1252)	7	
Rota rod test (seconds)						
Control	2.5±0.8	8	193	4.0±1.8	8	207
Edaravone 1.5 mg/kg/h	1.0±0.0 (p=0.3505)	8		2.7±0.4 (p=0.9782)	7	
Edaravone 3.0 mg/kg/h	3.3±1.5 (p=0.7336)	7		13.1±8.2 (p=0.2356)	7	
Inclined plate test (degree)						
Control	35.0±1.9	8	192	38.1±2.5	8	208
Edaravone 1.5 mg/kg/h	35.6±1.1 (p=0.8007)	8		41.4±1.4 (p=0.3126)	7	
Edaravone 3.0 mg/kg/h	39.3±1.7 (p=0.1840)	7		44.3±2.3 (p=0.1444)	7	

Values are mean ± SEM.

n=Number of animals.

* p < 0.05 vs. control group (Dunnett's test).

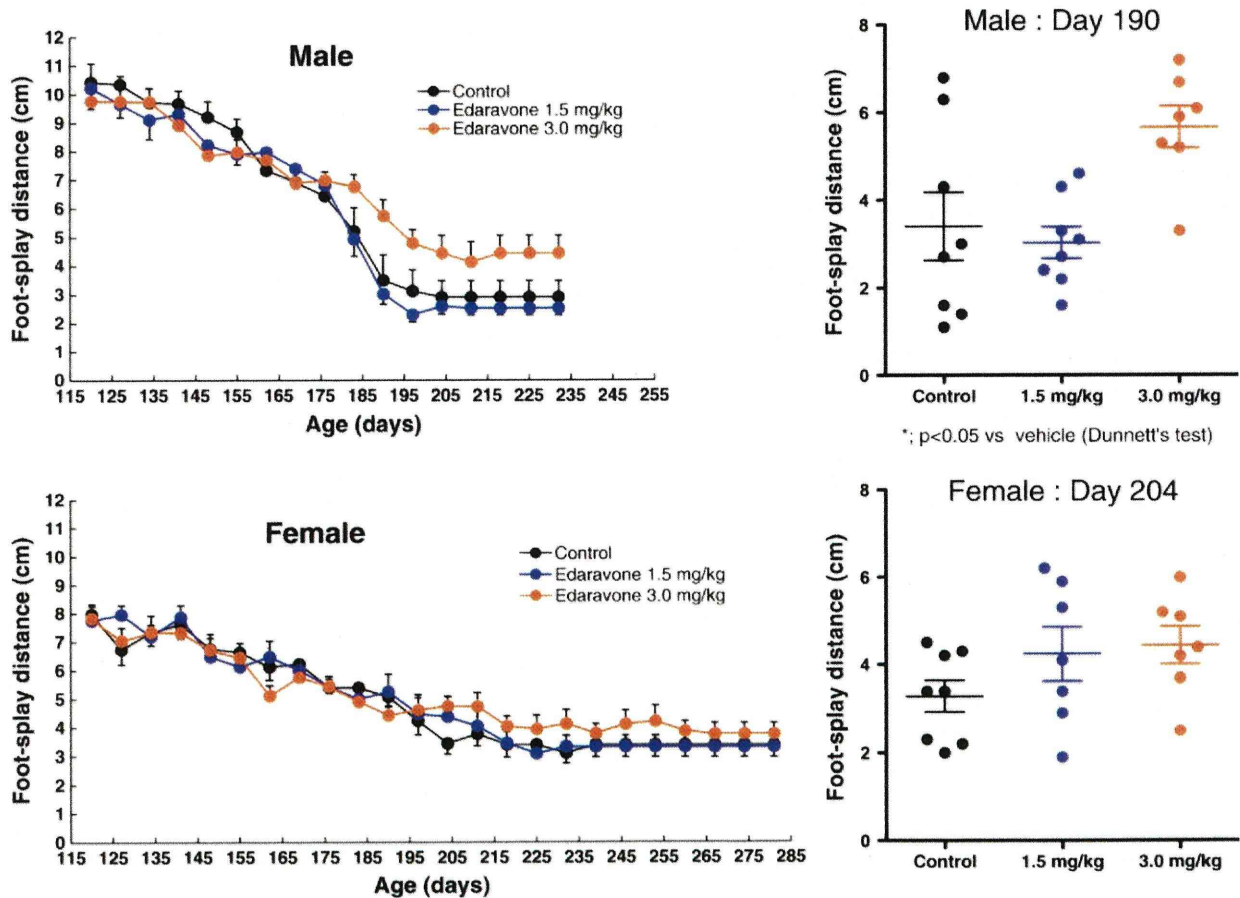


Fig. 2 – Effect of edaravone in the landing foot-splay test at 190 days in males and 204 days in females. The edaravone (3.0 mg/kg)-treated male group showed a significant improvement. Values are mean ± SEM of 7–8 animals. *p < 0.05 vs. control group (Dunnett's test).

the control, edaravone low-dose and edaravone high-dose group were $35.0 \pm 1.9^\circ$, $35.6 \pm 1.1^\circ$ and $39.3 \pm 1.7^\circ$ for males, and $38.1 \pm 2.5^\circ$, $41.4 \pm 1.4^\circ$ and $44.3 \pm 2.3^\circ$ for females, respectively. Edaravone dose-dependently tended to improve the sustainable angle in both males and females, but the differences did not reach statistical significance (Table 1).

3. Discussion

The transgenic rats we used in this study display adult-onset motor neuron disease (MND) with later onset, slower progression, and less variability in the phenotype than Gly93Ala (G93A) transgenic rats (Nagai et al., 2001; Matsumoto et al., 2006). The onset of clinical phenotype (about 24 weeks of age) is delayed by approximately 4.5 weeks in the present transgenic rats compared with the original H46R transgenic line (Nagai et al., 2001), presumably as a result of multiple passage.

Yoshino and Kimura (2006) found a beneficial effect of edaravone in a phase II clinical trial with ALS patients, who received edaravone intravenously (1-h infusion per day) for 14 days followed by a 14-day drug holiday for a total of 6 months. This regimen was based on that approved for acute cerebral infarction in Japan, i.e., 30-min infusion twice a day for 14 days. The modification of 30-min infusion twice a day to 1-h infusion once per day was made to improve the acceptability of long-term intravenous treatment. Interpolation of the 14-day drug holiday allowed repeated treatment cycles to be well tolerated. This regimen is also being used in an ongoing phase III study in Japan. After preliminary experiments based on the above regimens (data not shown), we chose continuous infusion (1 h per day) for 2 days followed by a 2-day holiday for the present animal study; this sequence was continued from 18 weeks of age to the day of loss of righting reflex.

Edaravone tended to extend both lifetime and duration of illness with apparent dose dependence, although the changes did not reach statistical significance. In the case of motor function evaluation, the results in the hind-foot reflex test, rota rod and inclined plate test tended to show an improvement with high-dose edaravone in both sexes, and in the landing foot-splay test, there was a statistically significant improvement in males. The tests were conducted throughout the treatment period, but we used the values at the time by which half of the control animals had died for statistical comparison, because this has the advantage of providing an objective time point for comparison. Although observed differences did not reach statistical significance in most cases, presumably due to the small sample size, our results at least suggest that the battery of motor functional measurements chosen for this rat model is appropriate.

The motor functional assessments we selected are commonly used for functional examination of animal models (Classen et al., 1994; Fischer and Peduzzi, 2007; Ding et al., 2004). Both the hind-foot reflex test and the landing foot-splay test measure reflex function, while the rota rod test measures coordinated movement of arms and legs, and the inclined plate test measures muscular strength of the four limbs. We could not identify the mechanism of action of edaravone in this study. However, there is a report that edaravone

treatment suppresses the progression of disuse muscle atrophy and improves leg locomotor function in acute stroke patients (Naritomi et al., 2010). Therefore, further studies to elucidate the action mechanism of edaravone on both nerve and muscle function in this model would be of interest.

Ito et al. (2008) reported that edaravone significantly improved motor functions, but not survival, in G93A SOD1 transgenic female mice. In our model, edaravone also did not improve survival but produced a significant improvement in the landing foot-splay test in male rats. Thus, edaravone but may ameliorate loss of motor function in SOD1 transgenic animals.

In conclusion, our battery of functional tests in the H46R SOD1 transgenic rat model seems to be useful for investigating candidate therapeutic agents for treatment of ALS, although most of the differences did not reach statistical significance, probably because of the small numbers of animals used in this exploratory study. Further studies to evaluate the efficacy of edaravone in this model with a larger number of animals seem worthwhile.

4. Experimental procedures

H46R SOD1 transgenic (Tg) rats of both sexes were used. Transgenic rats hemizygous for H46R mutation were crossed with wild-type Sprague–Dawley (SD) rats (Slc:SD; Japan SLC, Inc., Shizuoka, Japan) to produce transgenic and non-transgenic offspring. The transgenic progeny was genotyped by polymerase chain reaction amplification of tail DNA with specific primers for exon 4 (Nagai et al., 2001). All rats were handled according to approved animal protocols in our institution. All rats had free access to food and water throughout the experimental period.

4.1. Functional assessments

We defined the onset of disease as the day of the first observation of postural change in one limb when the rat was lifted by the tail (hind-foot reflex test). Death was defined as the day when the righting reflex disappeared. All functional measurements were done by a person blinded as to drug treatment. Briefly, the methods used were as follows.

4.1.1. Hind-foot reflex test

The animal was lifted by the tail and held suspended downward. Extension of the limbs was scored as follows: 0, all limbs fully extended (normal); 1, one limb bent; 2, two limbs bent; 3, three limbs bent; 4 all limbs bent. This test was carried out three times per week from 17 weeks of age.

4.1.2. Landing foot-splay test

The hind feet were coated with stamp-pad ink, then the animal was held from the back with both hands, with its body parallel to the landing point, and dropped from a height of approximately 30 cm over a landing foot-splay distance recording form. Landing foot-splay distance was defined as the distance between the hind feet measured between the heel imprints. This test was carried out once weekly from 17 weeks.

4.1.3. Rota rod test

The animal was placed on a rotarod (9 cm diameter, 8 cm wide; KN-75, Natsume Seisakusho Co., Ltd.) rotating at 5 rpm in the forward direction, and the longest time that the animal remained on the rod before falling was measured. The animals were trained twice or third times per week before symptoms, and the animals that could remain over 5 min on the cylinder were chosen for this experiment. This test was carried out once weekly from 17 weeks.

4.1.4. Inclined plate test

The animal was placed, pointing upward, on an inclined board set at 55°, 50°, 45°, 40°, 35°, or 30° gradient, and the angle at which the animal could remain without slipping for 5 s or more was determined. The test was started at 55°. From the second test on, measurement was started from one gradient setting higher than the maximum angle the animal had tolerated in the previous test. This test was carried out once weekly from 17 weeks of age.

4.2. Drug administration

Edaravone (1.5 or 3.0 mg/kg/h, male: $n=8$, female: $n=8$, in each group) or saline (male: $n=8$, female: $n=8$) was administered intravenously to rats by continuous infusion (1-h infusion per day) via a catheter. The catheter was inserted into the jugular vein, tunneled under the skin, and exteriorized on the dorsal surface of the neck to permit a continuous infusion of rats while allowing free movement.

The dosing regimen we chose was 2 days of administration followed by 2 days of drug holiday. This sequence was started at 18 weeks of age and repeated until the day of loss of righting reflex.

4.3. Statistical analysis

Lifetime and duration of illness were analyzed by applying the log-rank test. Survival was also plotted according to the Kaplan–Meier method. Statistical evaluation of motor function (hind-foot reflex test, landing foot-splay test, rota rod test and inclined plate test) was conducted for the data obtained at the nearest day and the previous day to that by which half of the control animals had died. Landing foot-splay and rota rod test results were analyzed with Dunnett's test, and hind-foot reflex and inclined plate test results with Steel's test.

REFERENCES

- Abe, K., Yuki, S., Kogure, K., 1988. Strong attenuation of ischemic and postischemic brain edema in rats by a novel free radical scavenger. *Stroke* 19, 480–485.
- Aoki, M., Ogasawara, M., Matsubara, Y., Narisawa, K., Nakamura, S., Itoyama, Y., Abe, K., 1993. Mild ALS in Japan associated with novel SOD mutation. *Nat. Genet.* 5, 323–324.
- Classen, W., Gunson, D.E., Iverson, W.O., Traina, V.M., Vonau, M.H., Krinke, G.J., 1994. Functional and morphological characterization of neuropathy induced with 5-lipoxygenase inhibitor CGS 21595. *Exp. Toxicol. Pathol.* 46, 119–125.
- Ding, Y., Li, J., Lai, Q., Rafols, J.A., Luan, X., Clark, J., Diaz, F.G., 2004. Motor balance and coordination training enhances functional outcome in rat with transient middle cerebral artery occlusion. *Neuroscience* 123, 667–674.
- The Edaravone Acute Infarction Study Group, 2003. Effect of a novel free radical scavenger, edaravone (MCI-186), on acute brain infarction. Randomized, placebo-controlled, double-blind study at multicenters. *Cerebrovasc. Dis.* 15, 222–229.
- Fischer, F.R., Peduzzi, J.D., 2007. Functional recovery in rats with chronic spinal cord injuries after exposure to an enriched environment. *J. Spinal Cord Med.* 30, 147–155.
- Gurney, M.E., Pu, H., Chiu, A.Y., Dal Canto, M.C., Polchow, C.Y., Alexander, D.D., Caliendo, J., Hentati, A., Kwon, Y.W., Deng, H.X., Chen, W., Zhai, P., Sufit, R.L., Siddique, T., 1994. Motor neuron degeneration in mice that express a human Cu, Zn superoxide dismutase mutation. *Science* 264, 1772–1775.
- Ito, H., Wate, R., Zhang, J., Ohnishi, S., Kaneko, S., Ito, H., Nakano, S., Kusaka, H., 2008. Treatment with edaravone, initiated at symptom onset, slows motor decline and decreases SOD1 deposition in ALS mice. *Exp. Neurol.* 213, 448–455.
- Matsumoto, A., Okada, Y., Nakamichi, M., Nakamura, M., Toyama, Y., Sobue, G., Nagai, M., Aoki, M., Itoyama, Y., Okano, H., 2006. Disease progression of human SOD1 (G93A) transgenic ALS model rats. *J. Neurosci. Res.* 83, 119–133.
- Mizuno, A., Umemura, K., Nakashima, M., 1998. Inhibitory effect of MCI-186, a free radical scavenger, on cerebral ischemia following rat middle cerebral artery occlusion. *Gen. Pharmacol.* 30, 575–578.
- Nagai, M., Aoki, M., Miyoshi, I., Kato, M., Pasinelli, P., Kasai, N., Brown Jr., R.H., Itoyama, Y., 2001. Rats expressing human cytosolic copper–zinc superoxide dismutase transgenes with amyotrophic lateral sclerosis: associated mutations develop motor neuron disease. *J. Neurosci.* 21, 9246–9254.
- Naritomi, H., Moriwaki, H., Metoki, N., Nishimura, H., Higashi, Y., Yamamoto, Y., Yuasa, H., Oe, H., Tanaka, K., Saito, K., Terayama, Y., Oda, T., Tanahashi, N., Kondo, H., on behalf of the MARVELOUS (Muscular Atrophy Restraint with Vigilant Edaravone Long-term Use after Stroke) Study Group, 2010. Effects of edaravone on muscle atrophy and locomotor function in patients with ischemic stroke: a randomized controlled pilot study. *Drugs R D* 10, 155–163.
- Reaume, A.G., Elliott, J.L., Hoffman, E.K., Kowall, N.W., Ferrante, R.J., Siwek, D.F., Wilcox, H.M., Flood, D.G., Beal, M.F., Brown Jr., R.H., Scott, R.W., Snider, W.D., 1996. Motor neurons in Cu/Zn superoxide dismutase-deficient mice develop normally but exhibit enhanced cell death after axonal injury. *Nat. Genet.* 13, 43–47.
- Rosen, D.R., Siddique, T., Patterson, D., Figlewicz, D.A., Sapp, P., Hentati, A., Donaldson, D., Goto, J., O'Regan, J.P., Deng, H.X., Rahmani, Z., Krizus, A., McKenna-Yasek, D., Cayabyab, A., Gaston, S.M., Berger, R., Tanzi, R.E., Halperin, J.J., Herzfeldt, B., Van den Bergh, R., Hung, W.Y., Bird, T., Deng, G., Mulder, D.W., Smyth, C., Laing, N.G., Soriano, E., Pericak-Vance, M.A., Haines, J., Rouleau, G.A., Gusella, J.S., Horvitz, H.R., Brown, R.H., 1993. Mutations in Cu/Zn superoxide dismutase gene are associated with familial amyotrophic lateral sclerosis. *Nature* 362, 59–62.
- Watanabe, T., Yuki, S., Egawa, M., Nishi, H., 1994. Protective effects of MCI-186 on cerebral ischemia: possible involvement of free radical scavenging and antioxidant actions. *J. Pharmacol. Exp. Ther.* 268, 1597–1604.
- Yoshino, H., Kimura, A., 2006. Investigation of the therapeutic effects of edaravone, a free radical scavenger, on amyotrophic lateral sclerosis (Phase II study). *Amyotroph. Lateral Scler.* 7, 241–245.

Human Hepatocyte Growth Factor Promotes Functional Recovery in Primates after Spinal Cord Injury

Kazuya Kitamura^{1,2,3}, Kanehiro Fujiyoshi¹, Jun-ichi Yamane¹, Fumika Toyota⁴, Keigo Hikishima^{2,4}, Tatsuji Nomura⁴, Hiroshi Funakoshi⁵, Toshikazu Nakamura⁶, Masashi Aoki⁷, Yoshiaki Toyama¹, Hideyuki Okano^{2*}, Masaya Nakamura^{1*}

1 Department of Orthopedic Surgery, Keio University School of Medicine, Shinjuku-ku, Tokyo, Japan, **2** Department of Physiology, Keio University School of Medicine, Shinjuku-ku, Tokyo, Japan, **3** Department of Orthopedic Surgery, Hiratsuka City Hospital, Hiratsuka, Kanagawa, Japan, **4** Central Institute for Experimental Animals, Miyamae-ku, Kawasaki, Kanagawa Japan, **5** Center for Advanced Research and Education, Asahikawa Medical University, Midorigaoka, Asahikawa, Japan, **6** Kringle Pharma Joint Research Division for Regenerative Drug Discovery, Center for Advanced Science and Innovation, Osaka University, Osaka, Japan, **7** Department of Neurology, Tohoku University School of Medicine, Sendai, Miyagi, Japan

Abstract

Many therapeutic interventions for spinal cord injury (SCI) using neurotrophic factors have focused on reducing the area damaged by secondary, post-injury degeneration, to promote functional recovery. Hepatocyte growth factor (HGF), which is a potent mitogen for mature hepatocytes and a mediator of the inflammatory responses to tissue injury, was recently highlighted as a potent neurotrophic factor in the central nervous system. We previously reported that introducing exogenous HGF into the injured rodent spinal cord using a herpes simplex virus-1 vector significantly reduces the area of damaged tissue and promotes functional recovery. However, that study did not examine the therapeutic effects of administering HGF after injury, which is the most critical issue for clinical application. To translate this strategy to human treatment, we induced a contusive cervical SCI in the common marmoset, a primate, and then administered recombinant human HGF (rhHGF) intrathecally. Motor function was assessed using an original open field scoring system focusing on manual function, including reach-and-grasp performance and hand placement in walking. The intrathecal rhHGF preserved the corticospinal fibers and myelinated areas, thereby promoting functional recovery. *In vivo* magnetic resonance imaging showed significant preservation of the intact spinal cord parenchyma. rhHGF-treatment did not give rise to an abnormal outgrowth of calcitonin gene related peptide positive fibers compared to the control group, indicating that this treatment did not induce or exacerbate allodynia. This is the first study to report the efficacy of rhHGF for treating SCI in non-human primates. In addition, this is the first presentation of a novel scale for assessing neurological motor performance in non-human primates after contusive cervical SCI.

Citation: Kitamura K, Fujiyoshi K, Yamane J-i, Toyota F, Hikishima K, et al. (2011) Human Hepatocyte Growth Factor Promotes Functional Recovery in Primates after Spinal Cord Injury. *PLoS ONE* 6(11): e27706. doi:10.1371/journal.pone.0027706

Editor: Cesario V. Borlongan, University of South Florida, United States of America

Received: June 30, 2011; **Accepted:** October 23, 2011; **Published:** November 29, 2011

Copyright: © 2011 Kitamura et al. This is an open-access article distributed under the terms of the Creative Commons Attribution License, which permits unrestricted use, distribution, and reproduction in any medium, provided the original author and source are credited.

Funding: This work was supported by grants from Grants-in-Aid for Scientific Research from JSPS and the Ministry of Education, Culture, Sports, Science and Technology of Japan (MEXT), the Project for Realization of Regenerative Medicine and Support for the Core Institutes for iPS Cell Research from MEXT, and by a grant-in-aid for the Global COE program from MEXT to Keio University. The funders had no role in study design, data collection and analysis, decision to publish, or preparation of the manuscript.

Competing Interests: The authors have declared that no competing interests exist.

* E-mail: masa@a8.keio.jp (MN); hidokano@a2.keio.jp (HO)

Introduction

Spinal cord injury (SCI) is followed by secondary degeneration, which is characterized by progressive tissue necrosis. Many experimental interventions have focused on this posttraumatic inflammatory process, using neurotrophic factors to reduce the damaged area and to promote axonal regeneration through the lesion epicenter. Neurotrophins such as nerve growth factor (NGF) [1,2], brain-derived neurotrophic factor (BDNF) [3], neurotrophin-3 (NT-3) [4,5], and glial cell line-derived neurotrophic factor (GDNF) [6,7] have been reported to enhance axonal growth in the injured spinal cord; some of these studies also showed that neurotrophins promoted behavioral recovery after SCI [3,7]. Both neurotrophic support and angiogenesis are critical to the endogenous regenerative response to trauma after SCI [8,9]. The initial damage to local blood vessels is decisive for the progression of destructive events during secondary degeneration [10], and strategic

treatments to improve angiogenesis after SCI have shown a relationship between blood flow and functional recovery [11,12].

Hepatocyte growth factor (HGF) was first identified as a potent mitogen for mature hepatocytes [13,14] and a natural ligand for the c-Met proto-oncogene product [15]. Recent studies have revealed that HGF acts as a neurotrophic factor for a variety of neuron types [16,17,18,19,20], and that administering HGF enhances angiogenesis, improves microcirculation, inhibits destruction of the blood-brain barrier [21], and exerts a neuroprotective effect after cerebral ischemia [22,23] and in the transgenic amyotrophic lateral sclerosis (ALS) rat model [24]. We previously reported that introducing exogenous HGF into the spinal cord significantly reduces the damaged area and promotes functional recovery in adult rats [25]. However, this strategy, which involved injecting a herpes simplex virus-1 vector into the spinal cord prior to SCI, can never be applied to clinical treatment. Furthermore, rodent SCI models are limited in their ability to ensure the efficacy

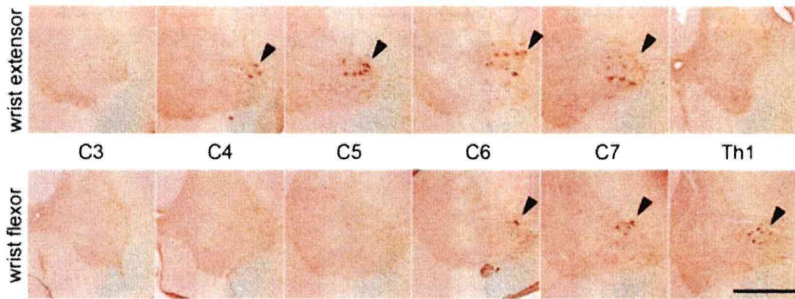


Figure 1. Retrograde labeling of motoneurons in the intact spinal cord by CTB injection. The motoneurons innervating the wrist and finger flexors and extensors were mainly distributed in lamina IX of the C4–C7 segments and the C6–Th1 segments, respectively. Almost all of these motoneurons were located at sites caudal to the lesion epicenter at the C5 level. Scale bar, 500 μm . doi:10.1371/journal.pone.0027706.g001

and safety of treatments for humans. It is critical to examine potential treatments in non-human primates before proceeding to clinical trials.

In this study, a total of 400 μg of recombinant human HGF (rhHGF) was infused intrathecally for four weeks immediately after C5-level contusive SCI in adult common marmosets, as a preclinical trial. Contusive injury is considered the most relevant to human SCI when evaluating therapies and predicting their translation to human treatment. However, to assess hand dexterity recovery, we needed an open field rating scale for a primate cervical SCI model that would be comparable to the BBB scale in rodents [26]. Therefore, we established an original open field rating scale to evaluate hand neurological performance after contusive cervical SCI. We found that intrathecal rhHGF infusion significantly reduced the areas of damaged tissue in the spinal cord and promoted functional recovery, consistent with our previous study using rats. This is the first study to report the efficacy and safety of rhHGF for SCI, and to present a novel scale for assessing neurological motor performance after contusive SCI in non-human primates.

Results

Distribution of the spinal motoneurons regulating wrist and finger motion in common marmosets

To precisely evaluate motor functions in the marmoset SCI model, we focused on the wrist and finger extension movements, because these motions are the most impaired in incomplete cervical SCI [27].

We first investigated the distribution of spinal motoneurons that innervate the hand muscles in marmoset forelimbs, by injecting cholera toxin B subunit (CTB) into the forearm flexor and extensor muscles. The wrist and finger extensor motoneurons were mainly located in lamina IX of the cervical (C)4–C7 segments, and wrist flexor motoneurons were in lamina IX of the C6–thoracic (Th)1 segments (Fig. 1). Based on these findings, we quantified the number of ChAT-positive motoneurons at these segments in marmosets treated with rhHGF or with sterile phosphate-buffered saline (PBS) after SCI. Twelve weeks after injury, the ChAT-positive motoneurons around the lesion epicenter had almost disappeared, consistent with our previous report [28], and we did not detect any significant differences in the number of surviving C2–Th1 ChAT-positive motoneurons between the two groups (data not shown).

rhHGF significantly preserved the corticospinal tract pathway and LFB-positive myelinated areas

We next investigated the pattern of the corticospinal tract (CST) pathway and its terminations in common marmosets. Axial sections of intact and injured spinal cords were immunostained with an anti-

calmodulin-dependent kinase II α (CaMK II α) antibody [29]. We previously found that CaMK II α -immunoreactivity (IR) labels the CST in the marmoset spinal cord [28,30,31], although its specificity remains to be demonstrated. In the present study, we made the following observations. First, in the intact spinal cord, CaMK II α -IR was detected in the lateral column of white matter, the dorsal horn, and the intermediate zone (IMZ) of the gray matter (Fig. 2A), suggesting that the CST in the common marmoset is located in lateral columns, unlike in rodents, in which the CST projects mainly to dorsal horn neurons and premotor spinal circuits [32]. Second, we did not detect CaMK II α -IR in either the ventral white matter column or the ventral gray matter horn, suggesting that, as in rodents, the proportion of the ventral CST extending into the white matter is small, and that the CST does not project directly to cervical motoneurons in the ventral horns.

Whereas CaMK II α -IR in the lateral column was obviously reduced in segments caudal to the lesion site in the PBS group compared with the intact spinal cord control, the CaMK II α -IR was well maintained, even caudal to the lesion site, in the rhHGF group (Fig. 2B arrowheads). Stereological quantification of the CaMK II α -positive area in the lateral column showed significant differences between the two groups at the segments caudal to the lesion site (Fig. 2D). CaMK II α -IR was detected in the IMZ (laminae VI–VII) cell bodies, which could include segmental interneurons (sINs) and propriospinal neurons (PNs). CaMK II α -positive neurons in the IMZ at C5 had disappeared at 12 weeks after SCI in both groups (Fig. 2B and C). The rhHGF group had obviously greater numbers of these neurons around the lesion epicenter, as compared with the PBS group (Fig. 2C). Quantitative analysis of these neurons showed significant differences between the two groups at the C4 and C6–Th1 segments (Fig. 2D). Note that in some segments, the number of neurons was greater in the rhHGF and PBS groups than in the intact spinal cord (Fig. 2D).

To examine rhHGF's tissue-sparing effects, we stained axial sections with Luxol fast blue (LFB) 12 weeks after SCI. There was a significant rim of spared myelinated white matter, even at the lesion epicenter, in the rhHGF group (Fig. 3A). Stereological quantitative analysis of the LFB-positive myelinated areas revealed significant differences around the lesion epicenter between the two groups (Fig. 3B). Significant differences were observed within one vertebral segment from the lesion site at the C5 level.

In vivo MRI and DTT findings reflected the histological severity of the spinal cord injury

In vivo MRI and diffusion tensor tractography (DTT) [30] were conducted at multiple time points (1, 3, and 12 weeks after SCI) in

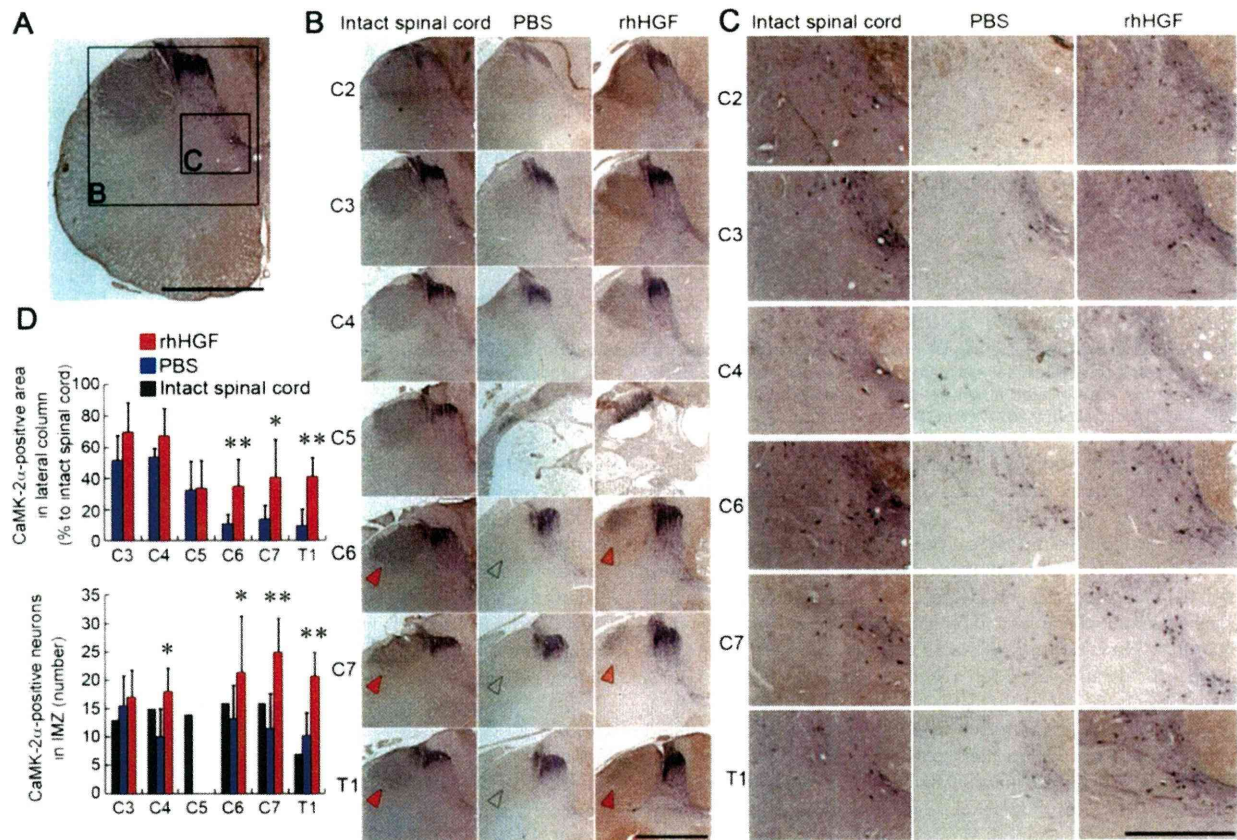


Figure 2. CaMK II α -immunoreactivity in the marmoset spinal cord. CaMK II α -immunoreactivity (IR) in the lateral column of the white matter and in the intermediate zone (IMZ) of the gray matter in an intact spinal cord (A) and injured spinal cord 12 weeks after SCI (B, C). (A) In the intact spinal cord, CaMK II α -IR was detected in the lateral column, dorsal horn and intermediate zone of the gray matter. No CaMK II α -IR was detected in the ventral horn of the gray matter. Scale bar, 1 mm. (B) CaMK II α -IR in the lateral column, suggesting the corticospinal tract (CST) pathway, was significantly preserved even at sites caudal to the lesion epicenter (arrowheads) in the rhHGF group compared with the PBS group. Scale bar, 1 mm. (C) CaMK II α -IR was detected in cell bodies at the IMZ (laminae VI–VII), suggested to be segmental interneurons and propriospinal neurons. There were significantly more IMZ CaMK II α -positive neurons at the C4 and C6–T1 segments in the rhHGF group than in the PBS group. IMZ CaMK2- α -positive neurons were absent from the C5 segment in both groups. Scale bar, 500 μ m. (D) Quantitative analyses of the CaMK II α -IR showed significant differences between the two groups. * $P < 0.05$, ** $P < 0.01$. (n = 6 for the rhHGF group; n = 5 for the PBS group; n = 1 for the intact spinal cord).

doi:10.1371/journal.pone.0027706.g002

four animals, two from each group that underwent SCI, to investigate *in vivo* images that might reflect the pathological changes after SCI. One animal from each group was subjected to MRI and DTT analysis on the same day, and the recovery of motor function was assessed over time using our open field rating scale. Sagittal T2-weighted images (T2WIs) from each individual showed a diffusely expanded high-intensity area around the lesion epicenter 1 week after SCI, which was gradually compacted thereafter with the low-intensity area inside (Fig. 4A). At 12 weeks after SCI, the area with abnormal intensity (low-intensity area surrounded by high-intensity area), suggesting a region of damaged parenchyma, was markedly reduced in the rhHGF-treated animal compared with the vehicle control animal (Fig. 4A). The axial T2WIs also showed marked reduction in the area with abnormal-intensity area. Note that the ventral and dorsal parts of the white matter in the rhHGF-treated animal showed normal intensity (Fig. 4B arrowheads) even at the lesion epicenter, whereas the abnormal T2-high intensity area in both the gray and white matter was greatly expanded in the vehicle control animal. The rhHGF-treated animal showed remarkable motor function

recovery beginning 3 weeks after SCI; until that point there were no obvious differences in the MRIs between the two animals (Fig. 4A and B), corresponding with the time of functional recovery as assessed by our original open field rating scale. The open field scores for the upper limbs of the rhHGF-treated animal and the vehicle control animal were, respectively, 3 and 6 at 3 weeks, and 14.5 and 6.5 at 12 weeks after SCI.

In vivo diffusion tensor analyses were performed at the same time points, and no obvious differences were observed between the two groups until 3 weeks after SCI (data not shown). At 12 weeks after SCI, DTT showed a larger number of spinal tract fibers around the lesion epicenter in the rhHGF group than in the PBS group, especially in the ventral white matter, which may have been a precise reflection of the spared rim of myelinated white matter detected by LFB staining and axial T2WIs (Fig. 5).

rhHGF did not give rise to abnormal CGRP-positive fiber outgrowth

Although allodynia-like withdrawal responses to mechanical stimulation of the four extremities were not observed after SCI in

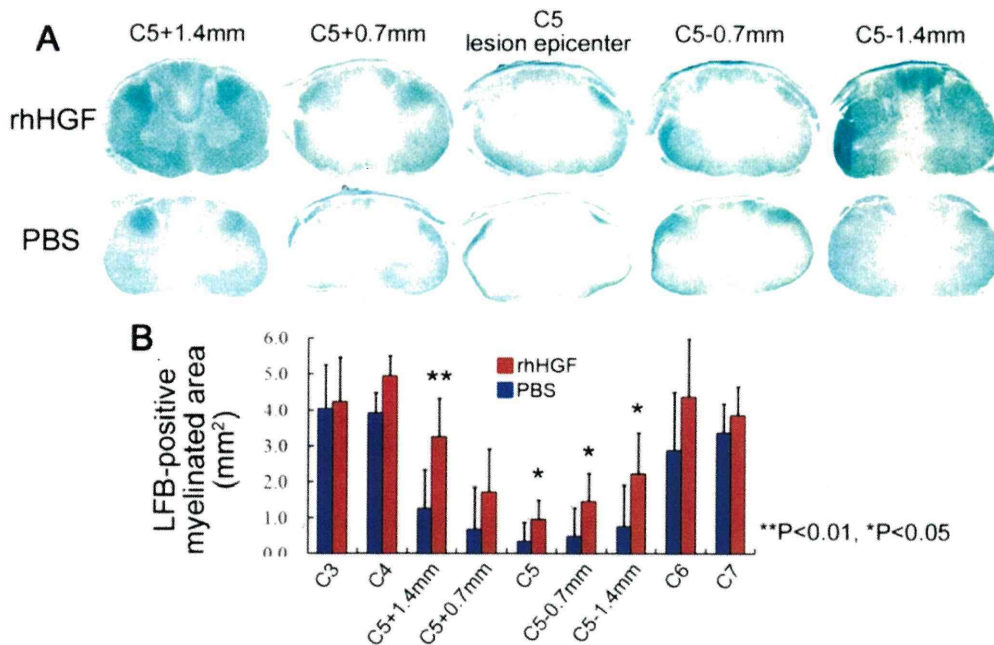


Figure 3. Significant reduction in the size of damaged parenchyma in the rhHGF group. Quantification of the LFB-positive myelinated area 12 weeks after SCI (A) showed a significant difference between the two groups around the lesion epicenter (B). Scale bar, 2 mm. ** $P < 0.01$, * $P < 0.05$, ** $P < 0.01$. (n = 6 for the rhHGF group; n = 5 for the PBS group). doi:10.1371/journal.pone.0027706.g003

either group, we quantified the calcitonin gene-related peptide (CGRP)-immunoreactive sensory axons in the Rexed lamina III 12 weeks after SCI to determine whether rhHGF treatment induced histological changes that could cause allodynia. Dense CGRP-positive innervation of lamina I and the outer part of lamina II was observed before and after SCI, and abnormal innervations of lamina III were detected after SCI in both groups (Fig. 6A). Stereological quantification of the total length of CGRP-positive fibers in lamina III revealed increased CGRP-positive

fiber length in both groups compared to the intact spinal cord, but did not show significant differences between the two groups rostrocaudal to the lesion epicenter at any site examined (Fig. 6B), suggesting that rhHGF treatment did not give rise to the abnormal sprouting of CGRP-positive nerve fibers.

Motor function recovery over time, original scale development, and category definitions

All animals showed severe quadriplegia 1 day after injury; they lay on the floor in a prone position, with little limb movement, and could not roll over or move forward by themselves. After C5-level SCI, irrespective of therapeutic intervention, the animals showed progressive recovery of motor function as assessed in three main categories: upper limbs, lower limbs, and trunk stability (Table 1). This study's injury model, cervical SCI, requires a detailed analysis of upper limb function to precisely evaluate motor function recovery. Thus, the upper limb category was divided into three subdivisions: weight bearing, reach and grip performance, and somatosensory function (Table 1). Because there were various combinations of improvement in multiple subdivisions and attributes, we adopted a point-addition scoring system in this original open field rating scale, unlike the system used in the BBB scale [26].

Weight bearing. The early phase of recovery was characterized initially by the animals' movement and placing of weight on the lower limbs. As the animals recovered, they showed slight to extensive movements of the three lower limb joints, and began to lift their upper body from the floor by bearing weight on the upper limbs in stance only. They also began to move forward by placing weight on the lower limbs, dragging the anterior chest on the floor without other observable movements, and placing weight on the upper limbs with the hands below shoulder level. The next phase of recovery was characterized by lifting the upper

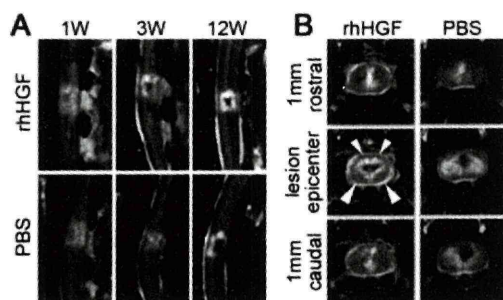


Figure 4. Representative MR images around the lesion epicenter after SCI, and correlation with functional recovery. (A) S Sagittal T2-weighted images around the lesion epicenter 1, 3, and 12 weeks after SCI. A marked reduction in the T2 low-signal-intensity area surrounded by a T2 high-signal-intensity area, suggesting cavity and glial scar formations, was detected in the rhHGF-treated animal compared with the vehicle control animal 12 weeks after SCI, even though there were no obvious differences between them up to 3 weeks after SCI. (B) Axial MR images around the lesion epicenter 12 weeks after SCI. The damaged T2 high-signal-intensity areas (arrowheads) were obviously reduced in the rhHGF-treated animal. doi:10.1371/journal.pone.0027706.g004

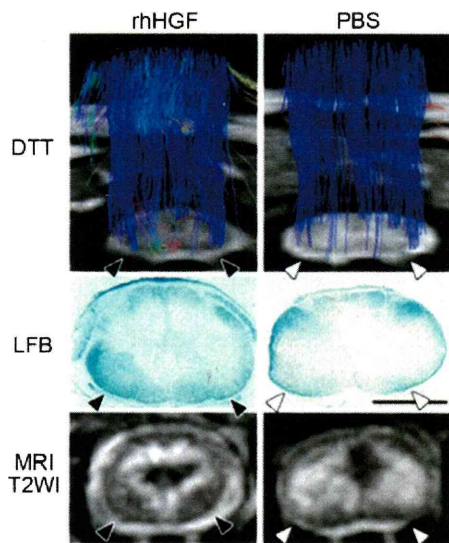


Figure 5. Diffusion tensor tractography (DTT) showing spinal fibers around the lesion epicenter, correlating with the histology and MR images. The region of interest (ROI) was placed in the upper cervical spinal cord, and full-width DTT of the spinal cord was traced in the caudal direction. Spinal fibers revealed by DTT in the ventral white matter (arrowheads) 12 weeks after SCI were correlated with the spared rim of LFB-positive myelinated area and the intact signal-intensity area in the axial T2-weighted images. Scale bar, 2 mm. doi:10.1371/journal.pone.0027706.g005

body by placing weight on the upper limbs, even when moving forward. When the animals progressed to raising the upper body from the floor in walking, they began to move their upper limbs to the rhythm of the walk, with their hands above shoulder level. However, more typically, the forearms were dragged on the floor, with the wrist joints dropped and the forearms not pronated. They were eventually able to bear weight on the upper limbs while walking, dragging only the hands, and finally recovered to walking without dragging the hands, in the most-recovered cases in the rhHGF group. The hand position also gradually recovered from being between the shoulder and head level to above the head. The most remarkable category, hand placement in walking, was assessed when the hands were above shoulder level, and was characterized by wrist extension, forearm pronation, and finger extension. Initially, the wrist joints were completely dropped, and the forearm was not pronated; thus, the animals supported their weight on the dorsal side of the hands (Fig. 7C) or on the ulnar side of the upper limbs. They eventually were able to extend the wrist joints, pronate the forearms, extend the fingers, and reestablish palmar contact with weight support (Fig. 7D); however no animals in the PBS group attained this level of recovery. The best performance was judged by the animal's ability to maintain a particular pattern throughout the testing session, not by its ability to exhibit a behavior once.

Reach-and-grasp performance. The assessment of reach-and-grasp performance highlighted finger flexion and extension, wrist extension, forearm pronation, and shoulder flexion. For several days after SCI, the animals could not raise their upper limbs, and could not actively flex their fingers even when a pen was placed in their hands. The animals eventually began to grasp a pen passively placed in their hands, and to lift their upper limbs to reach and grasp a pen that was suddenly presented in front of their eyes. They typically recovered the ability to elevate their hands up

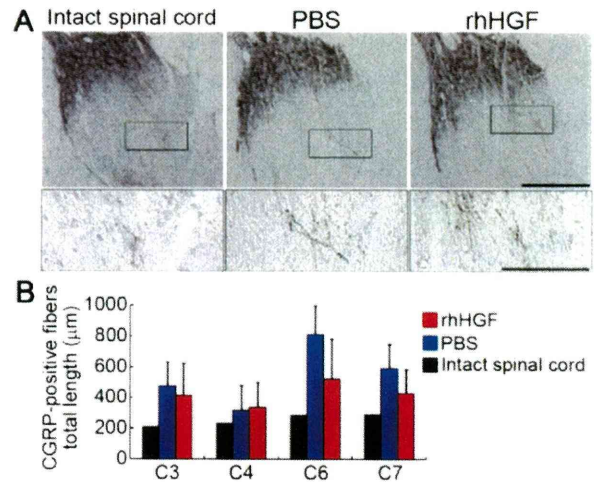


Figure 6. Quantitative analysis of CGRP-positive fibers at the dorsal horns. (A) Abnormal sprouting into lamina III at the dorsal horns was detected in both groups 12 weeks after SCI. Scale bar, 200 μm upper, 100 μm lower. (B) Quantitative analysis of the total length of these abnormal fibers showed no significant differences between the two groups in any segment examined ($n = 6$ for the rhHGF group; $n = 5$ for the PBS group; $n = 1$ for intact spinal cord). doi:10.1371/journal.pone.0027706.g006

to head height, and to reach and grasp a pen perpendicular to the body plane, with incomplete extension of the fingers and wrist joint. Many animals did not recover sufficiently to grasp a pen parallel to the body plane, even at head height (Fig. 7A), because it required full forearm pronation. They were also unable to elevate their hands to 3 cm above head height or to grasp pens in both directions, as this required active full shoulder joint flexion and full finger and wrist extension (Fig. 7B). In this assessment, the best performance was determined to be those attributes that were closest to normal behavior, even if they occurred only once.

Somatosensory function. Whereas intact animals never dropped their limbs through the gaps in the cage bars, animals after SCI often dropped the limbs through the floor gaps. We evaluated the distance the limb was dropped, as follows: lower limbs up to the thigh, knee, or foot only, and upper limbs up to the humerus, elbow, or hand only. Initially, the animals dropped their upper limbs up to the humerus and lower limbs up to the thigh, and were not able to raise the limbs at all (Fig. 7F). Over the course of motor recovery, they began to drop their upper limbs up to the elbow or only the hand, and lower limbs to the knee or only the foot (Fig. 7E). They also started pulling up the dropped limbs more quickly. Pulling up dropped limbs, which suggests somatosensory function recovery, was more likely to be observed in the lower than upper limbs. Somatosensory function was judged by the worst performance, even if it occurred only once.

rhHGF promoted significant motor function recovery

The bar grip (Fig. 8A) and spontaneous motor activity (Fig. 8B) [28,31,33] revealed significant motor function recovery in the rhHGF group. After SCI, the bar grip strength and spontaneous movements decreased sharply, and then recovered gradually. Spontaneous motor activity tests showed greater than 100% recovery in some animals in the rhHGF group around 8 weeks after SCI. At 12 weeks after SCI, the animals had recovered $62.4 \pm 2.6\%$ and $38.9 \pm 4.3\%$ of their bar-grip strength, and $77.8 \pm 12.7\%$ and $34.5 \pm 10.9\%$ of their spontaneous motor

Table 1. Original open field rating scale.

UPPER LIMBS maximum 20 points		
1. WEIGHT BEARING		
weight bearing in stance	anterior chest on the floor, no weight support of upperlimbs	+0
	anterior chest lifted up from the floor with weight support of upperlimbs	+1
weight bearing in walking	anterior chest on the floor, no weight support of upperlimbs	+0
	anterior chest lifted up from the floor with weight support of upperlimbs, with forearm dragged	+1
	with hand dragged	+1
	stepping with hand clearance from the floor	+1
	coordinated steps with lowerlimbs	+1
hand position in walking	below shoulder	+0
	between shoulder and head	+1
	above head	+1
hand placement in walking	dorsal placement (dropped wrist)	+0
	ulnar placement, not pronated	+1
	pronated, but no palmar placement	+1
	pronated with palmar placement	+1
2. REACH AND GRASP PERFORMANCE		
	elevation below head-height	+0
	cannot grasp a pen	+0
	grasp a pen	+1
	elevation up to head-height	+1
	cannot grasp a pen at head-height	+0
	grasp a pen perpendicular to the body plane	+1
	grasp a pen parallel to the body plane	+1
	elevation up to 3cm above head-height	+1
	cannot grasp a pen at 3 cm above head-height	+0
	grasp a pen perpendicular to the body plane	+1
	grasp a pen parallel to the body plane	+1
3. SOMATOSENSORY FUNCTION		
somatosensory	drop upper limbs through gaps in the cage bars up to	
	humerus	+0
	elbow	+1
	hand only	+1
	never drop	+1
TRUNK STABILITY maximum 3 points		
	cannot roll-over from supine to prone position	+0
	roll-over from supine to prone position	+1
	keep sitting position	+1
	keep standing position	+1
LOWER LIMBS maximum 7 points		
ROM & weight bearing	slight movement of lowerlimbs	+0
	extensive movement of lowerlimbs	+1
	move forward with weight bearing of lowerlimbs	+1
	jump	+1
	jump successively	+1
somatosensory	drop lower limbs through gaps in the cage bars up to	
	thigh	+0
	knee	+1

Table 1. Cont.

LOWER LIMBS maximum 7 points	
foot only	+1
never drop	+1

Definitions and abbreviations.

<UPPERLIMBS> **dorsal placement**: wrist joint is dropped and dorsal side of the hand is placed on the floor; **ulnar placement**: pronation of forearm is insufficient and little finger of the hand (ulnar side of the hand) is placed on the floor; **pronated, but no palmar placement**: forearm is pronated, wrist joint is extended, but no palmar placement due to limited fingers extension; **pronated with palmar placement**: palmar placement with forearm pronated and wrist and fingers extended
 <TRUNK STABILITY> **keep sitting or standing position**: keep sitting or standing position more than 5 seconds in the cage <LOWER LIMBS> **ROM**: range of motion; **slight movement of lowerlimbs**: partial joint movement through less than half of the range of the three joints motion; **extensive movement of lowerlimbs**: movement through more than half of the range of the three joints motion.

doi:10.1371/journal.pone.0027706.t001

activity, in the rhHGF and PBS groups, respectively. The evaluation of motor function by the original open field scale also showed significant differences between the two groups (Fig. 8C–E). Animals in both groups gradually recovered, reaching a plateau around 8 weeks after SCI, and the original score of the upper limbs (pre-injury score = 20) recovered to 15.9 ± 0.8 and 7.8 ± 1.8 in the rhHGF and PBS groups, respectively, 12 weeks after SCI (Fig. 8C). Significant differences between the two groups were observed at most time points from 12 days after SCI in the bar grip test, from 21 days after SCI in spontaneous motor activity, and from 14 days onward after SCI in the open field upper limb scores.

Validation of the original open field rating scale

Of the three methods assessing motor function (bar grip test, spontaneous motor activity, and open field scoring), our original open field rating scale yielded the smoothest recovery curve after SCI. Using this scale, the rating for the upper limbs showed a smoother recovery curve than that for lower limbs, reflecting the fact that the cervical SCI model used in this study is not a complete injury model, but rather a severe central cord syndrome model, which shows better and earlier functional recovery in the lower limbs than in the upper ones (Fig. 8C and D). To assess the validity of our open field scale, we evaluated its relationship to the anatomical lesions. Simple linear regression analyses showed that the original scale had more positive correlation with the quantitative histological analyses (Fig. 9A–C) than did the spontaneous motor activity test (Fig. 9D–F); the correlation was especially good with the CaMK II α -positive area [29] in the lateral column at Th1 (Fig. 8A; $R^2 = 0.785$), suggesting that the scale closely reflected the involvement of the CST pathway.

Discussion

We recently demonstrated that applying exogenous HGF by HSV-1 vector into the injured spinal cord of adult rats after SCI exerts significant neuroprotective and anti-apoptotic effects on neurons and oligodendrocytes to promote their survival, and enhances angiogenesis around the lesion epicenter. These multiple effects significantly reduce the area of damage and provide a better scaffold for axonal regeneration, thereby promoting functional recovery after thoracic SCI in rodents [25].

To begin to translate this HGF strategy to the treatment of human patients, here we performed intrathecal rhHGF infusion during the acute phase of cervical SCI in marmosets. Although previous clinical studies revealed that cervical SCI, which is more frequent in humans than SCI at other levels, is the main cause of manual dysfunction [34], a detailed examination of manual function following cervical SCI is difficult to obtain in rodents. A

major advantage of using non-human primates in translational research is the ability to assess fine motor control recovery in the forelimbs. Another advantage of using marmosets is the similarity of their neuroanatomy to that of human beings. Some features of motor projections have undergone pronounced changes from rodents to primates.

The CST is a major pathway for voluntary movement control. It is a phylogenetically new system that appeared first in mammals and developed predominantly in primates [35,36]. Over the course of the evolution of human and non-human primates, the CST has changed its location from the dorsal to lateral columns of the spinal cord [37] and changed its terminations. Whereas in rodents the CST axons project mainly to dorsal horn neurons and premotor spinal circuits, in primates, a significant proportion of the CST axons project to the ventral horn, and some synapse directly onto motoneurons innervating hand and forearm muscles, as direct cortico-motoneuronal (CM) connections [38].

Direct CM connections predominantly developed in higher primates such as macaque monkeys, apes, and humans [39,40,41]. Moreover, previous studies have suggested a strong correlation between the number of direct CM connections and the level of manual dexterity of non-human primate species [38,39,42,43]; the appearance of direct CM connections is correlated with the emergence of precision grip between the thumb and the index finger, which is observed in macaque monkeys but not in marmosets. Thus, macaque monkeys have been used in many experiments because they have more advanced finger dexterity than marmosets or squirrels. In previous experiments in macaque monkeys, a unilateral transection of the spinal cord was made to interrupt the CST, including direct CM connections, at the designated cervical segment, and the recovery of precision grip was assessed after SCI [44,45,46,47]. However, to evaluate and predict the therapeutic effects of interventions as human treatments, contusive injury is considered most relevant to human SCI. Furthermore, for precise assessments, the monkeys used in a translational study should be the same age, sex and body weight, which is problematic in experiments using macaque monkeys, but feasible in marmosets [48].

In this study, as shown in Figure 2, the CaMK II α -positive putative CST axons in marmosets were located in the lateral column, unlike in rodents, but projected mainly to the dorsal horn and IMZ without a visible CM connection, as in rodents, indicating the possibility that the marmoset CST is intermediate in the course of evolution from rodents to macaque monkeys and humans. Marmosets cannot perform a precise finger-thumb grip, but can be evaluated by reach-and-grasp prehensile tasks using a pen and by hand placement while walking. However, we could not evaluate these precise tasks using the previously reported bar grip

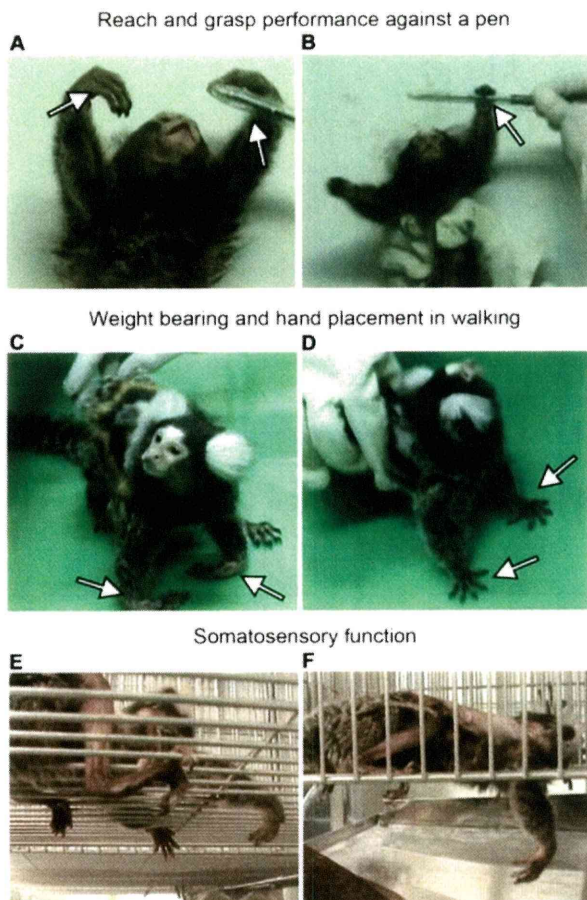


Figure 7. Representative images of marmosets after SCI. (A and B) An animal in the PBS group showed good elevation of upper limbs up to the head level 8 weeks after SCI. However, this animal could not grasp a pen parallel to the body plane because of insufficient forearm pronation and wrist and finger extension (A, arrowheads). An animal in the rhHGF group could reach for a pen at 3 cm above head height, and could grasp a pen even when parallel to the body plane. Note that the forearm was well pronated, with the wrist joint fully extended (B arrowhead). (C and D) The same animal as in (A) walked with the anterior chest lifted up from the floor by bearing its weight on the upper limbs. However, the wrist joints dropped completely, and the dorsal surfaces of the hands were placed and dragged on the floor (C arrowheads). On the other hand, the same animal as in (B) showed good palmar placement of the hands, with the wrist joints completely extended (D arrowheads), and walked with its hands clear of the floor. (E and F) One week after SCI, an animal in the PBS group dropped its limbs through gaps in the cage floor as far as the humerus or thigh, and could not raise the dropped limb quickly (F). The animal gradually recovered, and at 6 weeks after SCI, rarely dropped its limbs to the humerus or thigh level, but still often dropped them as far as the elbow or knee (E).
doi:10.1371/journal.pone.0027706.g007

test, cage-climbing test, or monitoring of spontaneous motor activity [31,33]. Furthermore, in the spontaneous motor activity test, some animals of the rhHGF group around 8 weeks after SCI showed activity that was more than 100% of the pre-injury level, suggesting that this test does not necessarily reflect neurological recovery. Therefore, we established an original open field rating scale, which enabled us to evaluate neurological hand performance after cervical SCI in marmosets. As shown in

Figure 1, almost all of the wrist extensor and flexor motoneurons were located at a site caudal to the lesion epicenter, suggesting the usefulness of evaluating wrist and finger extension and forearm pronation, which are important for performing reach-and-grasp prehensile tasks with a pen, and for hand placement while walking.

Intrathecal rhHGF infusion significantly reduced the damaged areas and promoted functional recovery after SCI, consistent with our previous report [25]. Although HGF's anti-apoptotic, neurotrophic, and angiogenic effects were not investigated during the acute phase of SCI [25] due to the small number of animals involved in this study, the LFB-positive myelinated areas and CaMK II α -positive fibers were significantly preserved in the rhHGF group. These effects resulted in significantly better neurological hand performance, which was successfully assessed by our original open field rating scale. Notably, our original open field scale had a better positive correlation with the CaMK II α -positive area in the lateral column at the Th1 level (Fig. 9A) and with the number of CaMK II α -positive IMZ neurons at T1 (Fig. 9B) than with the LFB-positive area at the C5 level (Fig. 9C), suggesting that it primarily reflects the neurological hand performance controlled by the CST. Furthermore, compared to the spontaneous motor recovery test (Fig. 9D-F) and bar grip test, our original open field scale (Fig. 9A-C) had more a greater positive correlation with the CaMK II α -positive area, CaMK II α -positive IMZ neurons and LFB-positive areas, suggesting that this open field rating scale more precisely reflects the neurological and pathological status after cervical SCI. However, the number of surviving ChAT-positive motoneurons, which innervate forearm muscles, showed no significant differences between the HGF-treated and control groups, in contrast with our previous reports. Based on this finding, it was necessary to reexamine the direct and indirect CM pathways after cervical SCI.

Compared with the direct CM pathway, the role of indirect pathways from the cerebral cortex to motoneurons, via subcortical or spinal interneuronal systems, has received much less attention, even though such pathways contribute the majority of motoneuron input [49]. In primates, many neuroanatomical studies have shown that the majority of corticospinal fiber terminations are not distributed in lamina IX, but in the IMZ of the spinal gray matter [50,51], where various types of interneurons are located. Intracellular recordings from motoneurons to investigate the effects of electrically stimulating the contralateral medullary pyramid (Pyr) in macaque monkeys suggest that PNs located in the C3-C4 segments can mediate the disynaptic excitation to motoneurons [52,53]. Furthermore, an evaluation of finger dexterity (precision grip with the tips of the index finger and thumb) suggests that the C3-C4 PNs play a significant role in recovering precision grip after a CST lesion at the border between C4 and C5, in which direct CM connections to forelimb motoneurons are interrupted, while a major portion of the of the C3-C4 PN descending axons (indirect CM connections) remain intact [44]. In contrast, precision grip does not recover after a CST lesion at C1/C2, which interrupts corticospinal input to the C3-C4 PNs [54]. These findings suggest that after a CST lesion at C4/C5, indirect CM connections can be used to control the reach-and-grasp hand movements requiring a precision grip in macaque monkeys.

In the present study, we induced a C5-level contusive injury as shown in Figure 2B; that is, caudal to the C3-C4 PNs and rostral to almost all forelimb motoneurons, as shown in Figure 1. This interrupted almost all the direct CM connections to forelimb motoneurons, whereas the majority of corticospinal input to the C3-C4 PNs remained intact, as shown in Figure 2. Therefore, this cervical SCI model is appropriate for investigating the involve-

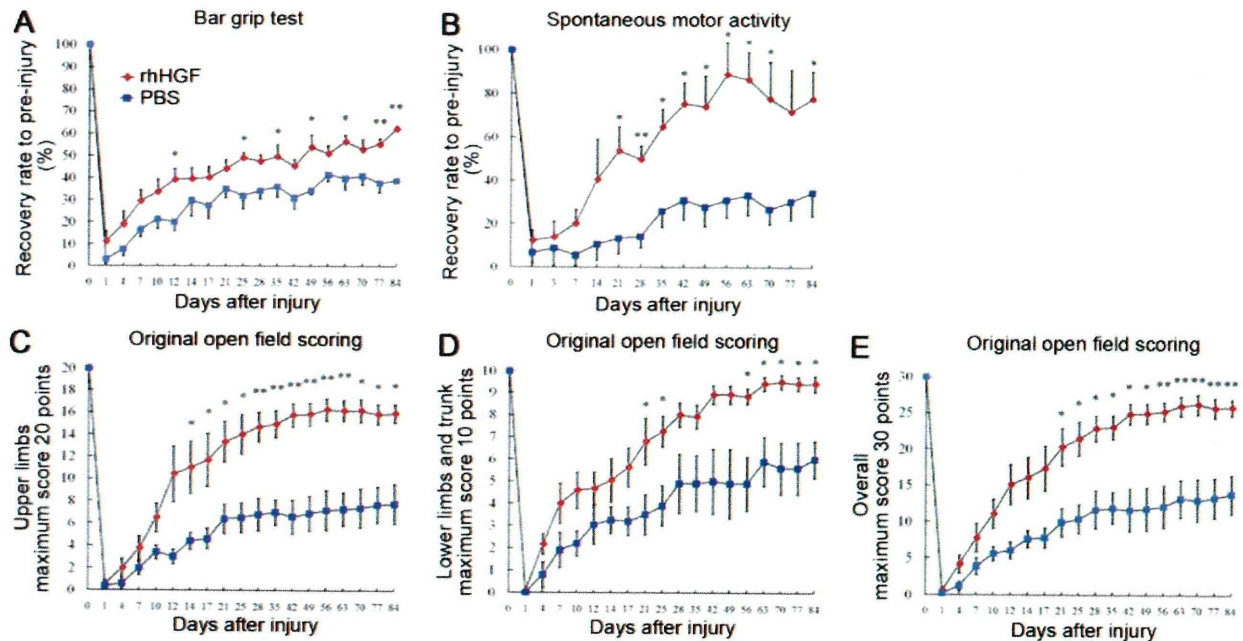


Figure 8. Functional recovery in rhHGF-treated marmoset SCI models. Behavioral analyses were performed by bar grip test (A), monitoring of spontaneous motor activity (B), and the original open field rating scale for the upper limbs (maximum, 20 points) (C), for the lower limbs and trunk (maximum, 10 points) (D) and combined (maximum 30 points) (E). All three methods showed significant recovery in the rhHGF group compared with the PBS group. Note that the original open field rating scale shows the smoothest recovery curve compared with the others. * $P < 0.05$, ** < 0.01 . (n = 6 for the rhHGF group; n = 5 for the PBS group). doi:10.1371/journal.pone.0027706.g008

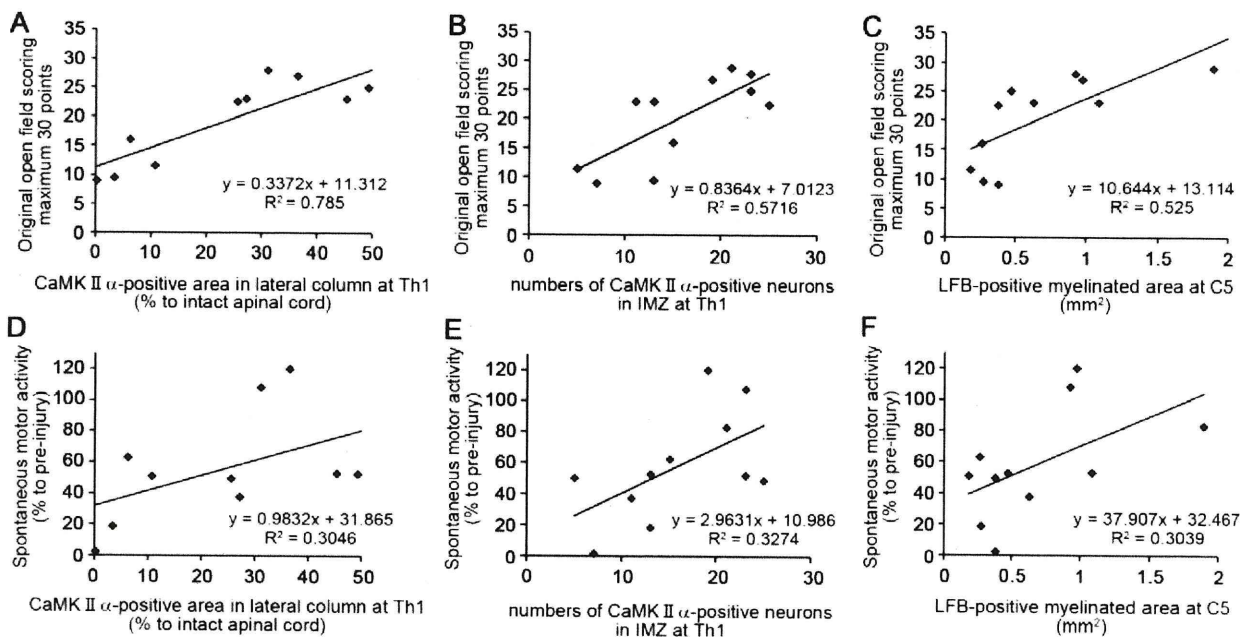


Figure 9. Relationship of the original open field scale and spontaneous motor activity to anatomical lesions. The original open field scale, with a maximum of 30 points, showed the greatest positive correlation with CaMK II α -positive areas in the lateral column at Th1 (A: $R^2 = 0.785$) and the next most positive correlation with CaMK II α -positive IMZ neurons at T1 (B: $R^2 = 0.5716$) compared with the four other correlations: the original open field scale and LFB-positive area at C5 (C: $R^2 = 0.525$), the spontaneous motor activity and CaMK II α -positive area in the lateral column at Th1 (D: $R^2 = 0.3046$), the spontaneous motor activity and CaMK II α -positive IMZ neurons at T1 (E: $R^2 = 0.3274$) and the spontaneous motor activity and LFB-positive area at C5 (F: $R^2 = 0.3039$). doi:10.1371/journal.pone.0027706.g009

ment and role of C3–C4 PNs in the recovery of hand dexterity. Significantly greater numbers of CaMK II α -positive interneurons in the IMZ at C4 and C6–Th1 segments were observed in the rhHGF group than the PBS group, suggesting that C3–C4 PNs played a major role in the recovery of hand movement after SCI in marmosets, as also described in macaques [44,46,47]. In spite of severe spinal cord damage around the lesion epicenter in the rhHGF group, motor function in the four extremities was recovered to a considerable extent, presumably by the endogenous plasticity of motor pathways, including indirect CM connections.

Beyond the CST, there are other possible mechanisms for functional recovery after SCI. First, the C3–C4 PNs could receive convergent inputs from various descending tracts, such as the rubro-, reticulo-, raphe-, and tectospinal tracts, as in rodents and cats [55,56,57]. Second, compared to rodents, primates engage more complex neural circuits in the parietal and frontal lobes of the cerebral cortex for even the simplest of skilled movements, suggesting that primates rely on the cortex for motor function [46,58,59,60,61,62]; this reliance could enable greater plasticity and recovery after SCI. Third, the reticulospinal tract, located in the ventral part of the spinal cord, controls both proximal and distal arm and hand muscles [63,64]. Experiments combining brain imaging with the pharmacological inactivation of motor cortical regions revealed time-dependent central compensatory mechanisms for finger dexterity after SCI in macaque monkeys; the recovery of finger dexterity involves the bilateral primary motor cortex during the early recovery stage, and more extensive regions of the contralesional primary motor cortex and bilateral premotor cortex during the late recovery stage [46]. In terms of clinical implications, these findings suggest that even limited sparing and regeneration of spinal projections after cervical SCI can be extremely beneficial to humans, enabling the recovery of some aspects of fine motor control.

With regard to clinical trials, methods for evaluating the spared and regenerating axons after SCI intervention are critical. If the extent and severity of the spinal cord lesion can be estimated by *in vivo* MRI techniques, including DTT [30], these analyses could provide strong predictive factors for functional recovery. In the present study, spinal tracts around the lesion site, revealed by DTT and by the intact intensity area in axial T2WI images, seemed to correlate with the spared rim of the LFB-positive myelinated area representing motor function recovery at 12 weeks after SCI; no obvious relationship between the *in vivo* images and motor function recovery was observed before 12 weeks. To improve the predictive and analytical value of these techniques, precise quantitative comparisons of *in vivo* MR images, pathological findings, and motor function over time after SCI will be necessary, especially during the acute phase of SCI (Konomi *et al.*, submitted).

We believe that intrathecal administration would also be the most effective administration route in the clinical application of rhHGF for SCI patients, because the blood-brain barrier significantly limits the translocation of rhHGF from blood to the spinal cord. We observed that the subcutaneous injection of rhHGF was ineffective in ALS rats (Funakoshi *et al.*, unpublished result), while the intrathecal administration of rhHGF showed significant therapeutic effects in these animals [24]. In the present study, we administered 400 μ g of rhHGF intrathecally over 4 weeks in marmosets, which corresponds to 0.05 mg/kg/day. Although we could not determine the HGF concentrations in the CSF of marmosets, we previously reported that the HGF levels in the spinal cord was elevated around 3-fold compared to the control level in SCI rats, when therapeutic effects of exogenous

HGF were observed [25]. Therefore, we assume that the enhancement of HGF concentration in the spinal cord to no more than 3-fold above the control level would be sufficient to show therapeutic effects, and there is probably no need to increase the HGF concentration to an extremely high level. The dosage to be used in clinical applications of HGF by intrathecal administration needs to be carefully assessed. Regarding the safety of intrathecal catheter insertion, infusion from the lumbar level has a great advantage over that from the cervical or thoracic level. Moreover, catheter insertion at the lumbar level might be useful for non-operated patients with SCI. This information needs to be assessed further to establish a therapeutic dose range and the optimal administration site for use in future clinical studies in SCI patients.

Overall, intrathecal rhHGF administration after SCI significantly reduced the extent of damage to the spinal cord parenchyma, preserved the CST pathway in the lateral column, and promoted hand dexterity, presumably by involving indirect CM pathways connected by interneurons. Furthermore, marmosets did not show abnormal behaviors or signs of discomfort or pain when the examiner touched their bodies or manipulated their limbs. These findings suggest that rhHGF treatment did not induce allodynia; this was also indicated by immunohistological analysis with an anti-CGRP antibody [65]. Taken together, the present study demonstrates the validity of our original open field behavior rating scale in a contusive cervical SCI model in primates, the efficacy and safety of intrathecal rhHGF treatment for SCI in adult non-human primates and the possibility that this novel therapy may be suitable for clinical application.

Materials and Methods

Preparation of osmotic mini-pump containing rhHGF or PBS

Osmotic mini pumps (Alzet model 2004; nominal pumping rate 0.25 μ l/hr, nominal duration 4 weeks, nominal reservoir 200 μ l, Alzet, CA, USA) were filled with PBS, or with rhHGF (Kringle Pharma, Inc., Osaka, Japan) diluted with PBS so that each pump contained 400 μ g of rhHGF. Each pump was connected to an intrathecal catheter (rat Intrathecal Catheter short; Alzet, CA, USA), and the apparatuses were incubated in sterile PBS at 37°C for 48 hours before use.

Contusive SCI and intrathecal infusion of rhHGF in common marmosets

Adult female common marmosets (295–350 g; Clea Japan, Tokyo, Japan) were used ($n=6$ for the rhHGF group; $n=5$ for the PBS group; $n=2$ for CTB injection; $n=1$ for intact spinal cord). All surgeries were performed under general anesthesia induced by intramuscular injection of ketamine (50 mg/kg; Sankyo, Tokyo, Japan) and xylazine (5 mg/kg; Bayer, Leverkusen, Germany) and maintained by isoflurane (Foren; Abbott, Tokyo, Japan). The animal's pulse, arterial oxygen saturation, and rectal temperature were monitored during the surgical procedures. After a laminectomy at the C5 level, the dura mater was exposed and a 20-g weight was dropped from a height of 50 mm onto the dura using a modified-NYU impactor as reported previously [28,31,33]. Right after contusive SCI at the C5 level, a C7 laminectomy was carried out and an intrathecal catheter was inserted from the C7 level. An osmotic mini pump, filled with 400 μ g rhHGF (HGF group) or PBS (control group) was connected to a catheter and placed in the subcutaneous space on the right side of the animal's back. The pump was left in place

to deliver the total 400- μ g dose of rhHGF for 4 weeks; dosage was based on previous results from intrathecal rhHGF administration in ALS rats [24], which have about the same body weight as marmosets. The animals were placed in a temperature-controlled chamber until thermoregulation was reestablished and received disinfectant treatment once a day. Manual manipulation of the fingers and joints in the four extremities was carried out twice a day and manual bladder expression was also performed twice a day until voiding reflexes were reestablished. Paralyzed animals were given adequate amounts of food and water until they recovered their ability to ingest food and water without assistance; thereafter, they had free access to food and water in the cage.

Ethics statement

All interventions and animal care procedures were performed in accordance with the Laboratory Animal Welfare Act, the *Guide for the Care and Use of Laboratory Animals* (National Institutes of Health, USA), the *Guidelines and Policies for Animal Surgery* provided by the Animal Study Committee of the Central Institute for Experimental Animals and Keio University and the guidelines outlined by Weatherall Report, and were approved by the Animal Study Committee of Keio University (IRB approval number 09091-8).

In vivo magnetic resonance imaging and diffusion tensor analysis

In vivo MRI and diffusion tensor studies were carried out at 1, 3, and 12 weeks after SCI in two animals from each group, four animals in total, under general anesthesia as described above. MRI was performed using a 7.0 tesla MRI, PharmaScan 70/16 (BioSpin; Bruker) with a coil dedicated for small animals; diffusion tensor analyses were performed as previously described [30]. The region of interest (ROI) was placed in the upper cervical spinal cord, and full-width DTT of the spinal cord was traced in the caudal direction.

Retrograde cervical motoneuron labeling by cholera toxin B subunit

Two intact animals were anesthetized with intramuscular injections of ketamine and xylazine as described above. A small skin incision was made in the left forearm of each, and 5 μ l of CTB (List Biological Laboratories, CA, USA) was manually injected into 4 points of the forearm flexor or extensor muscles. The animals were sacrificed 5 days after the CTB injection. Spinal cords were collected and immunohistological analysis performed as described below.

Histology

Spinal cords were perfusion-fixed with 4% paraformaldehyde in 0.1 M phosphate-buffered saline (PBS), and post-fixed in the same fixative (24 hr) with 10% sucrose in 0.1 M PBS (24 hr) and 30% sucrose in 0.1 M PBS (24 hr). Spinal cord segments were embedded in an optimal cutting-temperature compound and cut into 20- μ m-thick sections on a cryostat. For diaminobenzidine staining, the sections were incubated at 48°C with polyclonal anti-CaMK II α (CaMK II α ; 1:100; Zymed), polyclonal anti-CGRP (CGRP; 1:100; Affinity), and polyclonal anti-CTB (CTB; 1:500; Serotec) antibodies, followed by biotinylated secondary antibodies (1:500; Jackson ImmunoResearch). Biotinylated antibodies were visualized using the Vectastain Elite ABC kit (Vector Laboratories), followed by diaminobenzidine (Sigma). All images were obtained by microscopy (Axioskop 2 Plus; Zeiss, Oberkochen, Germany).

Stereology

To quantify the CaMK II α -positive area, LFB-positive myelinated area, and CGRP-positive fiber length, axial section images were obtained and analyzed using grain counting with light intensity by a Micro Computer Imaging Device (Imaging Research Inc., St. Catharines, Ontario, Canada). Threshold values were maintained at constant levels for all analyses. After obtaining images of axial sections stained with an anti-CaMK II α antibody, the number of CaMK II α -positive neurons in the intermediate zone (IMZ) of the gray matter was counted.

Behavioral analyses

Bar grip test. The bar grip test, which tests the animal's gripping reflex (the motion undertaken when attempting to grasp an object placed in front of their eyes) and evaluates the grip power, was carried out as previously reported [28,31,33]. The same device (220-mm wide, 500-mm deep, and 400-mm high, with a bar diameter of 2.5 mm in a 1 \times 3 [70 mm \times 100 mm] grid pattern) was used in the present study. The test was carried out three times a day. The percentage of the maximal grip strength relative to the mean strength before the injury was calculated on each day after the injury.

Spontaneous motor activity test. Spontaneous motor activity tests were carried out as previously reported [28,31,33]. We used cages (350-mm wide, 500-mm deep, and 500-mm high) equipped with infrared sensors (Murata Manufacturing Corp., Nagaokakyo, Kyoto, Japan) on the ceiling to continually record the marmosets' 3D motion. Our system utilized a passive thermographic infrared sensor to monitor heat emitted from the animals. The 3D localization of the heat source was monitored, and a change in this localization was recorded as movement. Each animal's data were recorded and monitored hourly on a computer, and the activity measured after the SCI was calculated as a percentage relative to that before the injury.

Original open field rating scale. To develop an original open field rating scale, the natural course of motor function recovery after cervical SCI was precisely observed in 6 marmosets before starting experiments using rhHGF. Two blinded examiners participated in all the open field tests and were positioned across from each other to observe both sides of the marmoset. Marmosets were tested alone for 5 minutes on the floor and in the cage 3 times per week until 4 weeks after SCI, and once per week thereafter. During the open field test, marmosets were encouraged by slight tapping when they remained stationary for longer than 15 seconds. In cases of borderline locomotor performance or disagreement between examiners, scores indicating the greater deficit were assigned. All lower limb movements were counted except those that were obviously part of a reflex (i.e., spastic extensive bilateral flexion, or extension of the hip, knee, or ankle joints). The bilateral upper limbs were assessed separately, and the score was defined as the mean of the bilateral scores for motor function.

Statistical analyses

All data are reported as the mean \pm SEM. In all the histological examinations, an unpaired two-tailed Student's t-test was used for single comparisons between the rhHGF and PBS groups. The results of the original open field rating scale, bar grip test, and spontaneous motor recovery test were analyzed using the Mann-Whitney U-test. To validate the original open field rating scale, correlations between the results of this scale and the spontaneous motor activity or histological findings (CaMK II α -positive areas in the lateral column at Th1, CaMK II α -positive neurons in IMZ and LFB-positive myelinated areas at C5) were analyzed by simple linear regression analyses.

53. Isa T, Ohki Y, Seki K, Alstermark B (2006) Properties of propriospinal neurons in the C3-C4 segments mediating disynaptic pyramidal excitation to forelimb motoneurons in the macaque monkey. *J Neurophysiol* 95: 3674–3685.
54. Isa T, Ohki Y, Alstermark B, Pettersson LG, Sasaki S (2007) Direct and indirect cortico-motoneuronal pathways and control of hand/arm movements. *Physiology (Bethesda)* 22: 145–152.
55. Pettersson LG, Lundberg A, Alstermark B, Isa T, Tantisira B (1997) Effect of spinal cord lesions on forelimb target-reaching and on visually guided switching of target-reaching in the cat. *Neurosci Res* 29: 241–256.
56. Pettersson LG, Perfiliev S (2002) Descending pathways controlling visually guided updating of reaching in cats. *Eur J Neurosci* 16: 1349–1360.
57. Illert M, Lundberg A, Padel Y, Tanaka R (1978) Integration in descending motor pathways controlling the forelimb in the cat. 5. Properties of and monosynaptic excitatory convergence on C3-C4 propriospinal neurones. *Exp Brain Res* 33: 101–130.
58. Schmidlin E, Wannier T, Bloch J, Rouiller EM (2004) Progressive plastic changes in the hand representation of the primary motor cortex parallel incomplete recovery from a unilateral section of the corticospinal tract at cervical level in monkeys. *Brain Res* 1017: 172–183.
59. Dancause N, Barbay S, Frost SB, Plautz EJ, Chen D, et al. (2005) Extensive cortical rewiring after brain injury. *J Neurosci* 25: 10167–10179.
60. Wannier T, Schmidlin E, Bloch J, Rouiller EM (2005) A unilateral section of the corticospinal tract at cervical level in primate does not lead to measurable cell loss in motor cortex. *J Neurotrauma* 22: 703–717.
61. Schmidlin E, Wannier T, Bloch J, Belhaj-Saif A, Wyss AF, et al. (2005) Reduction of the hand representation in the ipsilateral primary motor cortex following unilateral section of the corticospinal tract at cervical level in monkeys. *BMC Neurosci* 6: 56.
62. Belci M, Catley M, Husain M, Frankei HL, Davey NJ (2004) Magnetic brain stimulation can improve clinical outcome in incomplete spinal cord injured patients. *Spinal Cord* 42: 417–419.
63. Davidson AG, Buford JA (2006) Bilateral actions of the reticulospinal tract on arm and shoulder muscles in the monkey: stimulus triggered averaging. *Exp Brain Res* 173: 25–39.
64. Davidson AG, Schieber MH, Buford JA (2007) Bilateral spike-triggered average effects in arm and shoulder muscles from the monkey pontomedullary reticular formation. *J Neurosci* 27: 8053–8058.
65. Holstetter CP, Holmstrom NA, Lijja JA, Schweinhardt P, Hao J, et al. (2005) Allodynia limits the usefulness of intraspinal neural stem cell grafts; directed differentiation improves outcome. *Nat Neurosci* 8: 346–353.